2016

Genetic Requirement For The Rna Helicase Mov10l1 In Pirna Biogenesis

Qi Fu
University of Pennsylvania, fumister15@gmail.com

Genetic Requirement For The Rna Helicase Mov10l1 In Pirna Biogenesis

Abstract

GENETIC REQUIREMENT FOR THE RNA HELICASE MOV10L1 IN PIRNA BIOGENESIS

Qi Fu

P. Jeremy Wang

Piwi-interacting RNAs (piRNAs) are a class of small non-coding RNAs required for transposon silencing, germ cell development, and fertility in many eukaryotic species. However, many of the mechanisms underlying piRNA biogenesis have not been elucidated. Studies of MOV10L1 support its function as an RNA helicase in the processing of piRNA precursors. In this study, we elucidate the requirement for MOV10L1 RNA helicase activity in piRNA biogenesis.

To determine the requirement for MOV10L1 RNA helicase activity in piRNA biogenesis in vivo, we generated two knock-in mouse models containing mutations in residues of Mov10l1 that are critical for its RNA helicase activity. The two Mov10l1 knockin mutants displayed numerous phenotypes associated with impaired piRNA biogenesis. Adult male Mov10l1 knockin mutants exhibited meiotic arrest and sterility. piRNAs associated with the Piwi proteins MILI and MIWI2 were depleted in the Mov10l1 knockin mutants. The retrotransposons LINE1 and IAP were de-repressed in the germ cells of the Mov10l1 knockin mutants. Finally, the levels of piRNA precursor transcripts were upregulated in one of the Mov10l1 knockin mutants. Interestingly, the piRNA pathway proteins MOV10L1, MILI, and MIWI2 formed a polar conglomerate in the embryonic germ cells of the Mov10l1 knockin mutants, and MOV10L1 was not expressed post-natally in the Mov10l1 knockin mutants. Studies of the two Mov10l1 knockin mutants show that MOV10L1 RNA helicase activity is required for the processing of piRNA precursors and piRNA biogenesis.

Degree Type
Dissertation

Degree Name
Doctor of Philosophy (PhD)

Graduate Group
Cell & Molecular Biology

First Advisor
P. Jeremy Wang

Keywords
MOV10L1, piRNA, Piwi, RNA helicase, spermatogenesis

Subject Categories
Cell Biology | Genetics | Molecular Biology

GENETIC REQUIREMENT FOR THE RNA HELICASE MOV10L1 IN PIRNA

BIOGENESIS

Qi Fu

A DISSERTATION

in

Cell and Molecular Biology

Presented to the Faculties of the University of Pennsylvania

in

Partial Fulfillment of the Requirements for the

Degree of Doctor of Philosophy

2016

Supervisor of Dissertation

_____

P. Jeremy Wang, Professor of Developmental Biology,

Director, Center for Animal Transgenesis & Germ Cell Research

Graduate Group Chairperson

_____

Daniel S. Kessler, Associate Professor of Cell and Developmental Biology

Dissertation Committee

Mary Mullins, Professor of Cell and Developmental Biology

Chris Lengner, Assistant Professor of Cell and Developmental Biology

Brian Gregory, Associate Professor of Biology

George Gerton, Professor of Reproductive Biology in Obstetrics and Gynecology

ACKNOWLEDGMENT

I would like to thank the many people who have helped me get to this point. First and foremost, I would like to thank my PI, Jeremy Wang, for all the support he has given me throughout my graduate career. Jeremy has always pushed me to think creatively and has been there for me when I have needed guidance. He has provided me with numerous opportunities outside of the lab that have enhanced my graduate experience including writing a review and presenting my work at and attending multiple conferences.

I would also like to thank all the members of the Wang lab with whom I've worked with: Jian Zhou, Ke Zheng, Mengcheng Luo, Fang Yang, Seth Kasowitz, Jiangyang Xue, Yongjuan Guan, Yang Xu, and Baolu Shi for their friendship and support. In particular, I would like to thank Ke for taking the time and effort to train me when I first joined the Wang lab and for his continued guidance even after he left the lab. The time I've spent working in the Wang lab has helped me to improve as a scientist greatly and has encouraged me to pursue a career in biomedical research.

I would like to thank my committee members: Mary Mullins, Chris Lengner, Brian Gregory, and George Gerton for their guidance. They have provided unique and valuable opinions on my projects and have given me great advice for furthering my career as a scientist. I would also like to thank George Gerton for giving me the opportunity to be a mentor as part of the American Society of Andrology summer intern program. The experience taught me a great deal about teaching and communication.

I would like to thank the members of the Mourelatos lab at the University of Pennsylvania and the members of the Pillai lab at European Molecular Biology Laboratory with whom I have collaborated with throughout these years. I have never had

ii

any problems working with them, and their efforts have been critical to the success of my projects.

I would like to acknowledge the funding from the NIH/NICHD NRSA Fellowship that was used to support my projects, and I would like to thank the staff of the mouse vivarium at Hill Pavilion for taking care of my mice daily.

I am very appreciative of all the friends I have made during my time at the University of Pennsylvania and outside of the University of Pennsylvania who have supported me throughout this entire process. They have not only made my graduate school tenure fun and memorable, but as peers, they have also challenged me to become a better scientist. I am grateful that I had the opportunity to get to know all of them at some point in my life, and wish them all success in everything they do.

Last but not least, I would like to thank my parents: Ming Fu and Hongmei Ye, who have been unbelievable role models for me my entire life. They have provided me with the environment to thrive, pushed me to excel and at every step of the way, and have supported me during the highest and lowest points of my life. There are not enough words to describe how grateful I am to have the two of them in my life.

ABSTRACT

GENETIC REQUIREMENT FOR THE RNA HELICASE MOV10L1 IN PIRNA

BIOGENESIS

Qi Fu

P. Jeremy Wang

Piwi-interacting RNAs (piRNAs) are a class of small non-coding RNAs required for transposon silencing, germ cell development, and fertility in many eukaryotic species. However, many of the mechanisms underlying piRNA biogenesis have not been elucidated. Studies of MOV10L1 support its function as an RNA helicase in the processing of piRNA precursors. In this study, we elucidate the requirement for MOV10L1 RNA helicase activity in piRNA biogenesis.

To determine the requirement for MOV10L1 RNA helicase activity in piRNA biogenesis *in vivo*, we generated two knock-in mouse models containing mutations in residues of *Mov10l1* that are critical for its RNA helicase activity. The two *Mov10l1* knockin mutants displayed numerous phenotypes associated with impaired piRNA biogenesis. Adult male *Mov10l1* knockin mutants exhibited meiotic arrest and sterility. piRNAs associated with the Piwi proteins MILI and MIWI2 were depleted in the *Mov10l1* knockin mutants. The retrotransposons LINE1 and IAP were de-repressed in the germ cells of the *Mov10l1* knockin mutants. Finally, the levels of piRNA precursor transcripts were upregulated in one of the *Mov10l1* knockin mutants. Interestingly, the piRNA pathway proteins MOV10L1, MILI, and MIWI2 formed a polar conglomerate in the embryonic germ cells of the *Mov10l1* knockin mutants, and MOV10L1 was not expressed post-natally in the *Mov10l1* knockin mutants. Studies of the two *Mov10l1*

iv

knockin mutants show that MOV10L1 RNA helicase activity is required for the

processing of piRNA precursors and piRNA biogenesis.

v

TABLE OF CONTENTS

vii

ix

LIST OF TABLES

LIST OF ILLUSTRATIONS

CHAPTER 1. INTRODUCTION

Parts of this chapter were previously published in:

Fu, Q., and Wang, P.J. (2014). Mammalian piRNAs: Biogenesis, function, and mysteries. Spermatogenesis *4,* e27889.

Vourekas A, Zheng K, **Fu Q**, Maragkakis M, Alexiou P, Ma J, Pillai RS, Mourelatos Z, Wang PJ. 2015. The RNA helicase MOV10L1 binds piRNA precursors to initiate piRNA processing. *Genes Dev* **29**:617–629.

Overview

Piwi-interacting RNAs (piRNAs) are small, non-coding RNAs that play essential roles in transposon silencing, germ cell development, and fertility. The biogenesis of piRNAs is a complex process involving many components. Genetic studies of MOV10L1, a testis-specific, putative RNA helicase, have shown that it is required for the biogenesis of all mammalian piRNAs and the processing of piRNA precursors. In this study, we examine the function of MOV10L1 in piRNA biogenesis.

Reproduction and Fertility

Reproduction is essential for the survival of a species. Organisms pass their genetic and epigenetic information from one generation to the next through reproduction. Organisms that reproduce sexually such as humans produce specialized, haploid cells known as gametes. Male gametes are called sperm, and female gametes are called oocytes. A sperm and oocyte fuse together during fertilization to produce a single-celled,

1

diploid zygote. The zygote then develops into a multicellular organism that is able to produce its own gametes to continue the reproductive cycle.

Fertility is the ability of an organism to reproduce. Controlling fertility rates is important for maintaining global health. A survey by the Center for Disease Control from 2006-2010 estimated 6% of couples in the U.S. ages 15-44 suffered from infertility (Chandra et al., 2013). A survey by the World Health Organization estimated that infertility affected 13% of couples worldwide ages 20-44 in 2010 (Mascarenhas et al., 2012). Infertility can be attributed to problems with either sex or both sexes. For males, problems with infertility have also been associated with a higher risk of testicular cancer and a shorter life expectancy (Baker et al., 2005; Jensen et al., 2009; Jorgensen et al., 2011; Rives et al., 2012). On the other hand, another study estimated that 40% of pregnancies worldwide in 2012 were unplanned, and over half of these pregnancies ended in abortions or miscarriages (Sedgh et al., 2014).

Understanding the processes that regulate reproduction is vital for improving our ability to control fertility rates. In this study, we examine the functions of a protein that is involved in sperm development and required for male fertility in the mouse. The protein we are focusing on in this study and the processes underlying germ cell development are highly conserved among mammalian species. Therefore, the results of this study can be translated to humans.

Mouse spermatogenesis

Sperm are differentiated from diploid germ cells that undergo a series of developmental changes. The process is known as spermatogenesis (Figure 1.1). In mice, sperm are derived from primordial germ cells (PGCs) that first appear around embryonic day 7.25 (E7.25) (Ginsburg et al., 1990). PGCs migrate to and colonize the

2

genital ridges around E10.5 and start to proliferate (Molyneaux et al., 2001). During this period of PGC migration and proliferation, PGCs undergo genome-wide reprogramming where almost all DNA methyl marks are actively erased to reset the genome to a totipotent state (Sasaki and Matsui, 2008). PGCs are then specified to become male or female germ cells at E12.5 (Kocer et al., 2009). PGCs that are specified to become male germ cells are known as gonocytes and become mitotically inactive until after birth (Culty, 2013). During this window, gonocytes undergo *de novo* DNA methylation to establish sex specific DNA-methylation patterns (Smallwood and Kelsey, 2012).

After birth, gonocytes differentiate into spermatogonia to initiate the first wave of sperm production and at the same time establish a pool of spermatogonial stem cells to generate subsequent waves of sperm (Yoshida et al., 2006). Each wave of sperm production begins with the proliferation and differentiation of spermatogonia into spermatocytes. Spermatocytes then enter meiosis, a lengthy process where each diploid spermatocyte goes through two successive rounds of cell division, meiosis I and meiosis II, to give rise to four haploid, round spermatids that contain unique combinations of maternal and paternal DNA. During meiosis I, the primary spermatocyte divides into two secondary spermatocytes each containing a pair of sister chromatids. The prophase of meiosis I is the longest phase of meiosis and is split into four stages: leptotene, zygotene, pachytene, and diplotene. During this phase, homologous chromosomes pair together in a process called chromosomal synapsis and are able to exchange DNA through homologous recombination (Zickler and Kleckner, 1999). During meiosis II, the two secondary spermatocytes divide again, and the sister chromatids separate to generate four haploid, round spermatids. Round spermatids differentiate into functional sperm through a process known as spermiogenesis (de Kretser et al., 1998). Round spermatids first differentiate into elongated spermatids by condensing their nuclei and

3

forming an acrosomal cap to cover one side of the nucleus and a flagellum from the other side of the nucleus. Finally, elongated spermatids shed their cytoplasm to become mature sperm that are capable of fertilization.

Each wave of sperm production takes 35 days to complete in post-natal mice (Clermont, 1972). Sperm production occurs in structures that fill the testes called seminiferous tubules. Spermatogonia are located along the outer edges of the seminiferous tubules and differentiate into spermatocytes and spermatids as they migrate towards the center of the tubule. Elongated spermatids then travel down through the center of the tubule and into the epididymis where they undergo the final steps of maturation to become fully functional sperm. Spermatogenesis is strictly controlled to ensure that genetic and epigenetic information is correctly passed from one generation to the next.

Piwi-interacting RNAs

Germ cells use non-coding RNAs to control gene expression. Piwi-interacting RNAs (piRNAs) are an abundant class of small non-coding RNAs predominantly expressed in the germlines of many metazoans including C. elegans, Drosophila, zebrafish, silkworm, mouse, rat, and humans (Fu and Wang, 2014). piRNAs are 21-31 nucleotides (nt) long, contain a preference for a 5' uridine residue, and are 2'-*O*-methylated at their 3' ends. piRNAs associate with Piwi proteins, a subclass of the Argonaute protein family also predominantly expressed in the germline (Hock and Meister, 2008). The Argonaute protein family plays a central role in RNA silencing processes. Crystallization of full-length, archael Argonaute proteins and isolated domains of Argonaute proteins show they contain an RNase H-like fold with a conserved aspartate-aspartate-glutamate (D-D-H) catalytic motif that allows Argonaute proteins to

4

cleave their targets through the endonuclease/Slicer activity (Rashid et al., 2007; Rivas et al., 2005; Song et al., 2004; Yuan et al., 2005). Studies of piRNAs have shown that they are required for germ cell development and fertility in mice, Drosophila, and zebrafish (Khurana and Theurkauf, 2008). These studies show that piRNAs have played an essential role in germ cell development throughout evolution.

Transposable elements

The most well-characterized targets of piRNAs are transposable elements (TEs). The depletion of piRNAs in mice, Drosophila, and zebrafish resulted in a massive de-repression of TEs (Aravin et al., 2007; Brennecke et al., 2007; Houwing et al., 2007). Transposable elements (TEs) are selfish genetic elements that can move around and insert themselves randomly into the genome. They are present in most forms of life. Almost half of the human and mouse genomes are made up of TEs (Lander et al., 2001; Mouse Genome Sequencing Consortium et al., 2002). There are two major classes of TEs: DNA transposons and retrotransposons. The two classes of TEs are differentiated by the way they move around the genome. DNA transposons move through a "cut and paste" mechanism where they excise themselves from their original genomic location and insert themselves into a new genomic location. Retrotransposons move through a "copy and paste" mechanism. Retrotransposons are first transcribed into RNA intermediates. The RNA intermediates are then reverse-transcribed back into DNA by a reverse transcriptase. Finally, the newly synthesized retrotransposons are inserted into new genomic locations. While most TEs in human and mouse genomes are inactive due to accumulating mutations and truncations, a number of retrotransposons have remained active (Goodier and Kazazian, 2008). Retrotransposons, which make up the majority of TEs in the human and mouse genomes, can be divided into three main sub-

5

classes: retrotransposons containing long terminal repeats (LTRs), long-interspersed nuclear elements (LINEs), and short-interpersed nuclear elements (SINEs) (Lander et al., 2001; Mouse Genome Sequencing Consortium et al., 2002). LTR retrotransposons are autonomous elements that encode for proteins allowing them to self-propagate throughout the genome. LTR retrotransposons such as intracisternal particle A (IAP) retrotransposons are still active in mice, but not in humans (Moyes et al., 2007; Zhang et al., 2008). Subclasses of non-LTR retrotransposons include LINEs and SINEs. Like LTR retrotransposons, LINEs also encode for proteins that allow them to self-propagate throughout the genome. In contrast, SINEs are non-autonomous elements that can only be propagated using proteins encoded by active LINEs. LINE1 retrotransposons, the most abundant family of LINEs, make up 17-20% of mouse and human genomes (Lander et al., 2001; Mouse Genome Sequencing Consortium et al., 2002).

Deleterious effects of TE insertion

If left unchecked, TEs present a serious threat to genomic stability in cells. The insertion of TEs can cause genomic instability in a number of ways (Goodier and Kazazian, 2008). Direct insertion of a TE into a gene can disrupt its expression. TE insertion can also disrupt the expression of nearby genes by creating new splice sites, transcription factor binding sites, promoters, and adenylation signals. Additionally, TE insertion can lead to homologous recombination of non-allelic repeats, which can cause deletions, duplications, and other chromosomal rearrangements. To date, 65 diseases in humans have been attributed to TE insertions (Zamudio and Bourc'his, 2010). Hemophilia A was the first disease attributed to insertion of a LINE1 retrotransposon (Theophilus et al., 1998). TE insertions have also caused colon cancer, Huntington's disease, muscular dystrophy, etc. (Belancio et al., 2008). In mice, the deleterious effects

6

of TE insertions are even more pronounced. Around 10% of all mutations in mice were caused by insertion of a retrotransposon (Ostertag and Kazazian, 2001). The most successful TEs tend to only be expressed in germ cells, where *de novo* insertions can be passed on to future generations. Therefore, it is especially important to control transposon activity in germ cells. The piRNA pathway may have evolved in the germlines of animals as a way to combat active TEs and maintain genomic integrity.

piRNAs in mouse spermatogenesis

In mice, piRNAs are only essential for spermatogenesis and male fertility (Carmell et al., 2007; Deng and Lin, 2002; Kuramochi-Miyagawa et al., 2004; Lim et al., 2013). There are two populations of piRNAs expressed during mouse spermatogenesis: pre-pachytene and pachytene piRNAs (Figure 1.1). Both populations of piRNAs are required for spermatogenesis and male fertility. Pre-pachytene and pachytene piRNAs associate with three Piwi proteins: MILI, MIWI, and MIWI2, that display distinct expression patterns during spermatogenesis (Figure 1.1). *Mili* expression begins pre-natally in gonocytes immediately after sex determination and persists until the early round spermatid stage; *miwi2* expression begins pre-natally in gonocytes around E15 and persists in gonocytes until they differentiate into spermatogonia; finally, *Miwi* expression begins post-natally during the pachytene stage of meiosis and persists throughout the round spermatid stage (Aravin et al., 2008). MILI, MIWI, and MIWI2 associate with piRNAs of different lengths. MILI-bound piRNAs are 26nt long, MIWI2-bound piRNAs are 28nt long, and MIWI-bound piRNAs are 30nt long (Fu and Wang, 2014).

Pre-pachytene piRNAs are the first population of piRNAs generated during mouse spermatogenesis. They are first generated pre-natally in gonocytes and are

expressed until the onset of meiosis. Pre-pachytene piRNAs that are generated pre-natally associate with MILI and MIWI2 (Aravin et al., 2008). At E16.5, more than half of the piRNAs associated with MILI and MIWI2 are derived from transposon sequences, and a small percentage are also derived from genic sequences (Aravin et al., 2008). Pre-pachytene piRNAs generated after birth only associate with MILI. The composition of pre-pachytene piRNAs that are expressed post-natally changes. While the percentage of piRNAs derived from transposon sequences remains relatively similar at post-natal day 10, there is an increased percentage of piRNAs derived from SINEs and a decreased percentage of piRNAs derived from LTR retrotransposons and LINEs (Aravin et al., 2008). The percentage of piRNAs derived from genic sequences also increases at this stage (Aravin et al., 2008).

A much larger population of piRNAs, known as pachytene piRNAs, is generated post-natally in pachytene spermatocytes and is expressed until the round spermatid stage (Aravin et al., 2006; Girard et al., 2006; Grivna et al., 2006). Pachytene piRNAs constitute over 95% of piRNAs in the adult testis and associate with MIWI and MILI (Li et al., 2013). In contrast to pre-pachtyene piRNAs, only a minor fraction of pachytene piRNAs are derived from transposon sequences (Aravin et al., 2006; Girard et al., 2006; Grivna et al., 2006). Most pachytene piRNAs (>80%) are derived from intergenic sequences, and almost all pachytene piRNAs are located in clusters (Aravin et al., 2006; Girard et al., 2006; Grivna et al., 2006).

The next few sections describe the functions and biogenesis of piRNAs during mouse spermatogenesis. piRNAs have been understudied compared to other classes of small, non-coding RNAs such as transfer-RNAs and microRNAs, and additional studies are needed to fully understand their biology and functions. In this study, we examine mechanisms that underlie piRNA biogenesis.

8

Functions of pre-pachytene and pachytene piRNAs

Pre-pachytene and pachytene piRNAs play important but distinct roles in mouse spermatogenesis. Pre-pachytene piRNAs represent "traditional" piRNAs that are enriched for transposon-derived sequences. The depletion of pre-pachytene piRNAs results in a massive upregulation of TE activity and meiotic arrest. The depletion of pachytene piRNAs leads to round spermatid arrest but only has a minor effect on TE activity. The targets and functions of most pachytene piRNAs remain a topic of debate.

Tranposon silencing

Genome-wide reprogramming of PGCs erases repressive DNA methyl marks on TEs, providing a window of opportunity for TEs to propagate throughout the genome (Hajkova et al., 2002). The main function of pre-pachytene piRNAs is to silence active TEs in the germline during the period of *de novo* methylation that follows. The loss of pre-pachytene piRNAs in the testes of $Mili^{-/-}$ mice and $Miwi2^{-/-}$ mice resulted in the hypomethylation and increased expression of numerous LTR and LINE retrotransposons (Manakov et al., 2015). In particular, LINE1 and IAP retrotransposons displayed the highest levels of expression and hypomethylation in the testes of $Mili^{-/-}$ mice and $Miwi2^{-/-}$ mice and are commonly de-repressed in piRNA pathway mutants (Manakov et al., 2015; Yang and Wang, 2016). Examining the activity of LINE1 and IAP retrotransposons in the germ cells of piRNA pathway mutants shows that they are both de-repressed pre-natally in gonocytes, but exhibit binary de-repression patterns post-natally in spermatocytes and spermatogonia, respectively (Di Giacomo et al., 2013; Zheng et al., 2010). The impaired function of pachytene piRNAs also led to the de-repression of LINE1 retrotransposons in spermatocytes and round spermatids in *Miwi* mutant mice (Reuter et al., 2011). The

9

piRNA pathway silences active TEs at the transcriptional and post-transcriptional level. At the post-transcriptional level, the piRNA machinery processes TE-derived transcripts to generate piRNAs (Aravin et al., 2008). Pre-pachytene piRNAs guide MILI to endonucleolytically cleave *Line1* and *Iap* transcripts, and pachytene piRNAs guide MIWI to endonucleolytically cleave *Line1* transcripts (De Fazio et al., 2011; Reuter et al., 2011). At the transcriptional level, pre-pachytene piRNAs guide MIWI2 into the nucleus, where MIWI2 is required to establish DNA methyl marks on TEs during the period of *de novo* methylation (Aravin et al., 2008; Kuramochi-Miyagawa et al., 2008). It is hypothesized that MIWI2 recruits DNA methylation machinery to the sites of methylation. MILI also regulates the *de novo* methylation of a subset of TEs independently of MIWI2, but the mechanisms through which this occurs remain a mystery (Manakov et al., 2015). The effects of TE de-repression on germ cell development are detailed in the next two sections.

Meiosis

In most piRNA pathway mutants, defects in pre-pachytene piRNA biogenesis cause germ cell development to arrest at the leptotene/zygotene stage of meiosis I (Table 1.1). The onset of meiosis proceeds normally in the germ cells of these piRNA pathway mutants but chromosomal synapsis is impaired (Carmell et al., 2007; Kuramochi-Miyagawa et al., 2004; Soper et al., 2008; Zheng et al., 2010). A meiotic checkpoint is activated in response to the chromatin defects, which leads to meiotic arrest (Roeder and Bailis, 2000). There are multiple theories as to how TE de-repression could cause these chromatin defects. One theory is that the active LINE1 retrotransposons cause massive DNA damage in spermatocytes (Soper et al., 2008). Another theory is that the active LINE1 retrotransposons attract the recombination

10

machinery away from canonical recombination hotspots (Zamudio et al., 2015). The arrested germ cells are eventually cleared through apoptosis.

Spermiogenesis

In piRNA pathway mutants, defects in pachytene piRNA biogenesis cause germ cell development to arrest at the round spermatid stage (Table 1.1). Impaired pachytene piRNA function only leads to a modest de-repression of LINE1 retrotransposons, suggesting that the increased TE activity may not be responsible for round spermatid arrest (Reuter et al., 2011). Unlike pre-pachytene piRNAs, the majority of pachytene piRNAs do not display extensive complementarity with any other parts of the genome (Aravin et al., 2006). The functions and targets of these pachytene piRNAs has remained unclear. Initial studies of pachytene piRNAs suggested pachytene piRNAs directly or indirectly regulate the translation of spermiogenic RNAs (Castaneda et al., 2014; Zhao et al., 2013). Recent studies have shown that pachytene piRNAs are able to guide MIWI to cleave and/or silence meiotic and spermiogenic RNAs (Goh et al., 2015; Gou et al., 2014; Zhang et al., 2015). A *Miwi* mutant expressing a catalytically dead MIWI protein also exhibited round spermatid arrest, supporting the role for pachytene piRNAs in directing the cleavage of mRNAs by MIWI (Reuter et al., 2011).

piRNA biogenesis

piRNA biogenesis is required for transposon silencing, germ cell development, and fertility in numerous species. A great deal of effort has gone into identifying components required for piRNA biogenesis, but many of the mechanisms and functions of components involved in piRNA biogenesis have yet to be elucidated. piRNA biogenesis in mice has been particularly difficult to study compared to in other organisms

due to the lack of a system that allows for easy genetic manipulation. Uncovering mechanisms involved in piRNA biogenesis will help to reveal how the piRNA pathway regulates transposon activity and germ cell development.

Unlike microRNAs, piRNAs are generated in a Dicer-independent manner (Vagin et al., 2006). The majority of piRNAs in mice are located in clusters that can be tens to hundreds of kilobases in length (Li et al., 2013). piRNA clusters are transcribed by RNA Polymerase II into long, single-stranded RNAs, termed piRNA precursors, that contain H3K4me2 marks at their transcriptional start sites, 5' caps, and 3' poly-A tails. A-MYB is required for the transcription of pachytene but not pre-pachytene piRNA precursors (Li et al., 2013). piRNA precursors are then exported from the nucleus to perinuclear granules, termed nuages. How piRNA precursors are distinguished from other canonical RNA Polymerase II transcripts remains a mystery. The RNA-binding protein MAELSTROM is localized to both the nucleus and nuages and associates with pachytene piRNA precursors (Castaneda et al., 2014). MAELSTROM may be involved in exporting piRNA precursors from the nucleus to the nuages. The nuages are the sites of piRNA processing. In pre-natal gonocytes, piRNAs are processed in two, distinct nuages: the pi-body and piP-body (Aravin et al., 2009). Pi-bodies are small granules located between mitochondria. They are collectively termed the intermitochondrial cement (IMC). piP-bodies are larger granules that form adjacent to pi-bodies. piP-bodies disappear after birth, and piRNA processing continues in the IMC until the mid-late pachytene stage of meiosis. In round spermatids, pachytene piRNAs and other components of the piRNA pathway are located in a single, large granule known as the chromatoid body (Meikar et al., 2011). However, it is unclear as to whether piRNA processing occurs in the chromatoid body because certain components required for piRNA processing are not

12

expressed in round spermatids. piRNAs are processed via two pathways: primary biogenesis and the ping-pong cycle (Figure 1.2).

Primary biogenesis

Pre-pachytene and pachytene piRNAs are initially generated via primary biogenesis. During primary biogenesis, piRNA precursors are endonucleolytically cleaved into fragments that are loaded onto MILI and MIWI as piRNA intermediates. MITOPLD is a putative endonuclease. It is required for piRNA biogenesis in mammals and is thought to be responsible for the cleavage of piRNA precursors because its homolog, Zucchini, cleaves piRNA precursors in Drosophila (Ipsaro et al., 2012; Nishimasu et al., 2012; Watanabe et al., 2011). MOV10L1 is also required for the processing of piRNA precursors (Zheng and Wang, 2012). MILI- and MIWI-bound piRNA intermediates contain a preference for a 5' uridine residue (Vourekas et al., 2012). The 5' ends of piRNA intermediates are the same as mature piRNAs, but their 3' ends are longer than mature piRNAs (Vourekas et al., 2012). In Silkworm, piRNA intermediates are trimmed at their 3' ends to mature piRNA lengths by the exonuclease PNLDC1 (Trimmer), whose activity is dependent on its interaction with Papi (Izumi et al., 2016). MILI-bound piRNA intermediates also accumulated in the absence of TDRKH, the mouse homolog of Papi (Saxe et al., 2013). TDRKH directly interacts with MIWI in post-natal germ cells and partially co-localizes with MIWI2 in embryonic gonocytes (Saxe et al., 2013). TDRKH may act as a scaffold for Trimmer and the Piwi/piRNA intermediate complex. Finally, the 3' ends of piRNAs are 2'-*O*-methylated by the HEN1 methyltransferase (Lim et al., 2015). Additional components involved in primary biogenesis whose functions are unknown include GASZ, GPAT2, and HSP90 alpha (Table 1.1). Further studies are also needed to elucidate how piRNA precursors are

13

processed during primary biogenesis. This study explores the role of MOV10L1 in the processing of piRNA precursors.

Ping-pong cycle

The ping-pong cycle allows the piRNA pathway to create a more robust and adaptive defense against active TEs in the germline by coupling piRNA biogenesis with the *de novo* methylation of TEs. During the ping-pong cycle, MILI is involved in an intra-amplification loop that amplifies pre-natal, pre-pachytene piRNAs derived from LINE1 and IAP retrotransposons and also generates a pool of antisense, secondary piRNAs. First, LINE1- and IAP-derived piRNAs guide MILI to cleave a complementary RNA (De Fazio et al., 2011). MILI cleaves the target RNA at the 10th nucleotide relative to the 5' end of the piRNA to generate the 5' end of the secondary piRNA (Gunawardane et al., 2007; Martinez and Tuschl, 2004). Thus, a signature of secondary piRNAs is a preference for an adenine residue at the 10th nucleotide, which is lost in mice expressing a catalytically inactive MILI (De Fazio et al., 2011; Gunawardane et al., 2007). It is still unclear as to how secondary piRNAs are further processed and loaded onto Piwi proteins in mice. In Drosophila, the 5' ends of secondary piRNAs are loaded onto Piwi proteins, and then the 3' ends are either directly cleaved to mature piRNA lengths by Zucchini or cleaved to intermediate lengths by a Piwi protein and trimmed to mature piRNA lengths (Han et al., 2015; Mohn et al., 2015). The same mechanisms may regulate the loading and processing of secondary piRNAs in mice. Secondary piRNAs in mice are associated with either MILI or MIWI2. Secondary piRNAs associated with MILI guide MILI to cleave complementary RNAs to amplify LINE1- and IAP-derived piRNAs. MIWI2 Slicer activity is not required for piRNA biogenesis (De Fazio et al., 2011). Instead, secondary piRNAs associated with MIWI2 guide MIWI2 into the nucleus, where

14

MIWI2 is required for the methylation of LINE1 and IAP retrotransposons (Kuramochi-Miyagawa et al., 2008). Additional components involved in the biogenesis of secondary piRNAs whose functions are unknown include TDRD9, TDRD12, MAEL, EXD1, FKBP6, HSP90 alpha, and MVH (Table 1.1).

MOV10L1: a master regulator of piRNA biogenesis

The focus of this study is on the function of Moloney leukemia virus 10-like 1 (MOV10L1) in piRNA biogenesis. MOV10L1 is a testis-specific, putative RNA helicase. The C-terminal of MOV10L1 contains its RNA helicase domain while the N-terminal of MOV10L1 is not homologous to any known protein (Zheng et al., 2010). MOV10L1 is able to unwind double-stranded RNA in a 5'-3' direction *in vitro* (Vourekas et al., 2015). MOV10L1 is a homolog of ARMITAGE, which is required for piRNA biogenesis in Drosophila (Saito et al., 2010). *Mov10l1* displays the same expression pattern as *mili* during spermatogenesis (Frost et al., 2010). MOV10L1 associates with MILI, MIWI, and TDRD1 *in vivo* and *in vitro* (Zheng et al., 2010). Currently, MOV10L1 is one of the only known proteins required for the biogenesis of both pre-pachytene and pachytene piRNAs. MILI- and MIWI2-bound, pre-pachytene piRNAs were depleted in *Mov10l1*$^{\Delta/\Delta}$ mice expressing a truncated MOV10L1 protein in which part of the RNA helicase domain was deleted (Zheng et al., 2010). Male *Mov10l1*$^{\Delta/\Delta}$ mice exhibited numerous phenotypes commonly associated with a loss of pre-pachytene piRNAs including an arrest of germ cell development at the leptotene/zygotene stage of meiosis, impaired chromosomal synapsis, sterility, and de-repression of LINE1 and IAP retrotransposons (Zheng et al., 2010). MILI- and MIWI-bound pachytene piRNAs were depleted when *Mov10l1* was disrupted post-natally in leptotene/zygotene spermatocytes

15

using an Ngn3-Cre (Zheng and Wang, 2012). The expression of MILI-associated pre-pachytene piRNAs was not affected in *Ngn3cre;Mov10l1*^{fl/Δ} mice (Zheng and Wang, 2012). The depletion of pachytene piRNAs in *Ngn3cre;Mov10l1*^{fl/Δ} mice caused germ cell development to arrest at the round spermatid stage (Zheng and Wang, 2012). Interestingly, there was no significant de-repression of LINE1 retrotransposons in *Ngn3cre;Mov10l1*^{fl/Δ} mice (Zheng and Wang, 2012).

MOV10L1 is required for the processing of piRNA precursors: A model for MOV10L1 function

MOV10L1 is also required for the processing of piRNA precursors. The expression levels of several pachytene piRNA precursors were upregulated in *Ngn3cre;Mov10l1*^{fl/Δ} mice (Zheng and Wang, 2012). MOV10L1 directly associates with piRNA precursors (Vourekas et al., 2015). The majority of MOV10L1-bound RNA mapped to piRNA clusters, but only a small percentage of MOV10L1-bound RNA was mature piRNAs (Vourekas et al., 2015). The 5' ends of piRNA intermediates are protected by MILI and MIWI and are not susceptible to nucleolytic activity (Vourekas et al. 2012). In contrast, the 5' ends of MOV10L1-bound RNAs were cleaved when treated with RNase (Vourekas et al., 2015). The susceptibility of the 5' ends of MOV10L1-bound RNAs to nucleolytic activity suggests MOV10L1 binds to piRNA precursors before they are incorporated into Piwi proteins as piRNA intermediates. MOV10L1 binding sites on piRNA precursors were enriched near the 3' ends of MILI-and MIWI-bound piRNAs (Vourekas et al., 2015). MOV10L1 also associated with MITOPLD *in vitro* (Vourekas et al., 2015). The proximity of MOV10L1 binding sites to the 3' ends of piRNAs coupled with the interaction between MOV10L1 and MITOPLD suggests that MOV10L1 binding

16

onto piRNA precursors is coupled with the cleavage of piRNA precursors by MITOPLD to generate the 5' ends of piRNAs. MOV10L1-bound RNA also contained a high frequency of guanine residues that could lead to the formation of secondary structures such as G-quadruplexes (Vourekas et al., 2015). Bioinformatic analysis of G-quadruplex and secondary structure formation within piRNA precursors shows that these structures have a high potential to form within MOV10L1 binding sites (Vourekas et al., 2015). Furthermore, MOV10L1 is required to resolve G-quadruplexes within piRNA precursor transcripts, as G-quadruplexes were enriched in piRNA precursor transcripts in *Ngn3cre;Mov10l1*^{fl/Δ} mice (Vourekas et al., 2015)

Analysis of MOV10L1-bound RNA suggests a role for MOV10L1 as an RNA helicase in the processing of piRNA precursors (Figure 1.3). In this model, MOV10L1 translocates along the piRNA precursor in a 5'-3' direction and feeds the piRNA precursor to the piRNA machinery for processing. MOV10L1 forms a large complex with other components of the piRNA pathway including MILI, MIWI, and MITOPLD. MOV10L1 and the rest of the complex translocate along the piRNA precursor until it reaches a region containing a secondary structure, such as a G-quadruplex. As MOV10L1 is resolving the secondary structure, MITOPLD cleaves the piRNA precursor to generate the 5' ends of piRNAs. This cleavage event may also generate the 3' ends of the preceding piRNA precursor fragments. Cleaved piRNA precursors containing 5' uridine residues are then loaded onto MILI or MIWI as piRNA intermediates. MILI and MIWI dissociate from the complex after the loading of piRNA intermediates, which are further processed into a mature piRNAs. An empty Piwi protein associates with the complex after MILI or MIWI dissociates from the complex. Once the secondary structure

17

has been resolved, MOV10L1 and the rest of the complex continue to translocate along the piRNA precursor until it reaches a region containing another secondary structure.

Additional studies are needed to determine the precise molecular function of MOV10L1 in piRNA biogenesis. In this study, we address the requirement for MOV10L1 RNA helicase activity in piRNA biogenesis.

Thesis Objectives

Previous studies of MOV10L1 have shown that it is a master regulator of piRNA biogenesis and is required for the processing of piRNA precursors. MOV10L1 is a putative RNA helicase, but the requirement for its enzymatic activity in piRNA biogenesis has not been examined. I hypothesize that MOV10L1 RNA helicase activity is essential for its role in piRNA biogenesis. To test this hypothesis, we generated two *Mov10l1* mutants containing mutations in residues critical for MOV10L1 RNA helicase activity. In Chapter 3, we generate and characterize the phenotype of a knock-in mouse model containing a point mutation in the ATP binding motif of the MOV10L1 RNA helicase domain. In Chapter 4, we generate and characterize the phenotype of a knock-in mouse model containing a double point mutation in the ATP hydrolysis motif of the MOV10L1 RNA helicase domain. Ultimately, we are able to elucidate the requirement for MOV10L1 RNA helicase activity in piRNA biogenesis.

18

TABLES

Protein	Known roles in piRNA biogenesis	Mutant phenotype	References
PIWIL2 (MILI)	Primary and secondary piRNA biogenesis	Meiotic arrest	Kuramochi-Miyagawa et al. 2004, Aravin et al. 2006, De Fazio et al. 2011
PIWIL1 (MIWI)	Primary biogenesis	Spermiogenic arrest	Deng et al. 2002, Grivna et al. 2006
PIWIL4 (MIWI2)	Secondary piRNA biogenesis	Meiotic arrest	Carmell et al. 2007, Manakov et al. 2015
MOV10L1	Primary biogenesis	Meiotic arrest	Zheng et al. 2010, Zheng et al. 2012
DDX4 (MVH)	Secondary piRNA biogenesis	Meiotic arrest	Kuramochi-Miyagawa et al. 2010
TDRD1	Primary biogenesis	Meiotic arrest	Reuter et al. 2009, Chuma et al. 2006
TDRD9	Secondary piRNA biogenesis	Meiotic arrest	Shoji et al. 2009
TDRD12	Secondary piRNA biogenesis	Meiotic arrest	Pandey et al. 2013
TDRKH	Primary biogenesis	Meiotic arrest	Saxe et al. 2013
PLD6	Primary biogenesis	Meiotic arrest	Watanabe et al. 2011
ASZ1(GASZ)	Primary biogenesis	Meiotic arrest	Ma et al. 2009
MAEL	Primary and secondary piRNA biogenesis	Meiotic arrest	Soper at al. 2008, Aravin et al. 2009, Casteneda et al. 2014
FKBP6	Secondary piRNA biogenesis	Meiotic arrest	Xiol et al. 2012
Hsp90 alpha	Primary and secondary piRNA biogenesis	Meiotic arrest	Grad et al. 2010, Ichiyanagi et al. 2014
HENMT1	Primary biogenesis	Spermiogenic defect	Lim et al. 2015
GPAT2	Primary biogenesis	??	Shirimoto et al. 2013
EXD1	Secondary piRNA biogenesis	Fertile	Yang et al. 2016

Table 1.1: Roles of piRNA pathway proteins in piRNA biogenesis and mutant phenotypes.

19
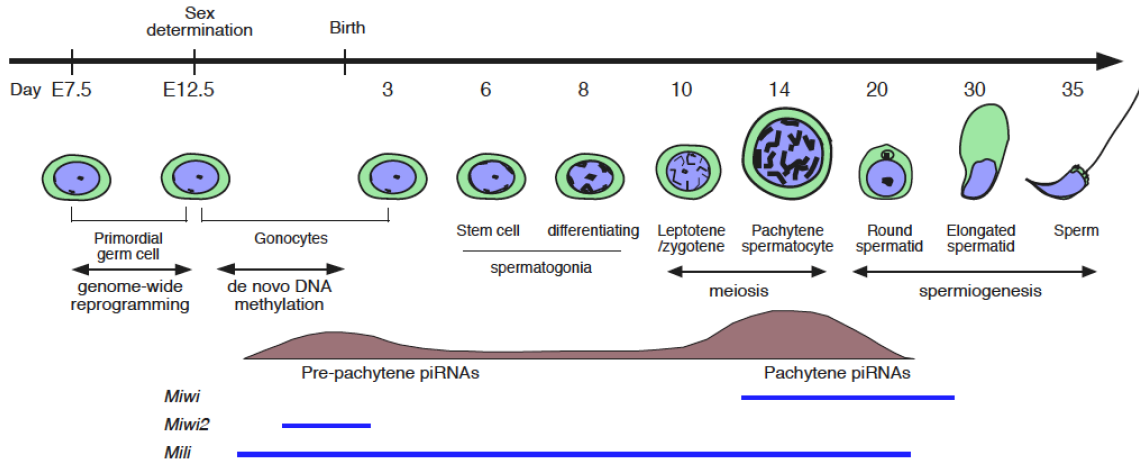
Figure1.1: Expression of piRNAs and Piwi proteins during mouse spermatogenesis. Illustration of key stages and events occurring during the first wave of mouse spermatogenesis beginning with the appearance of primordial germ cells and their maturation into spermatozoa. Subsequent waves of spermatogenesis originate from spermatogonial stem cells. The tan histogram represents the expression patterns of pre-pachytene and pachytene piRNAs throughout spermatogenesis. The blue lines represent the expression patterns of MILI, MIWI2, and MIWI.
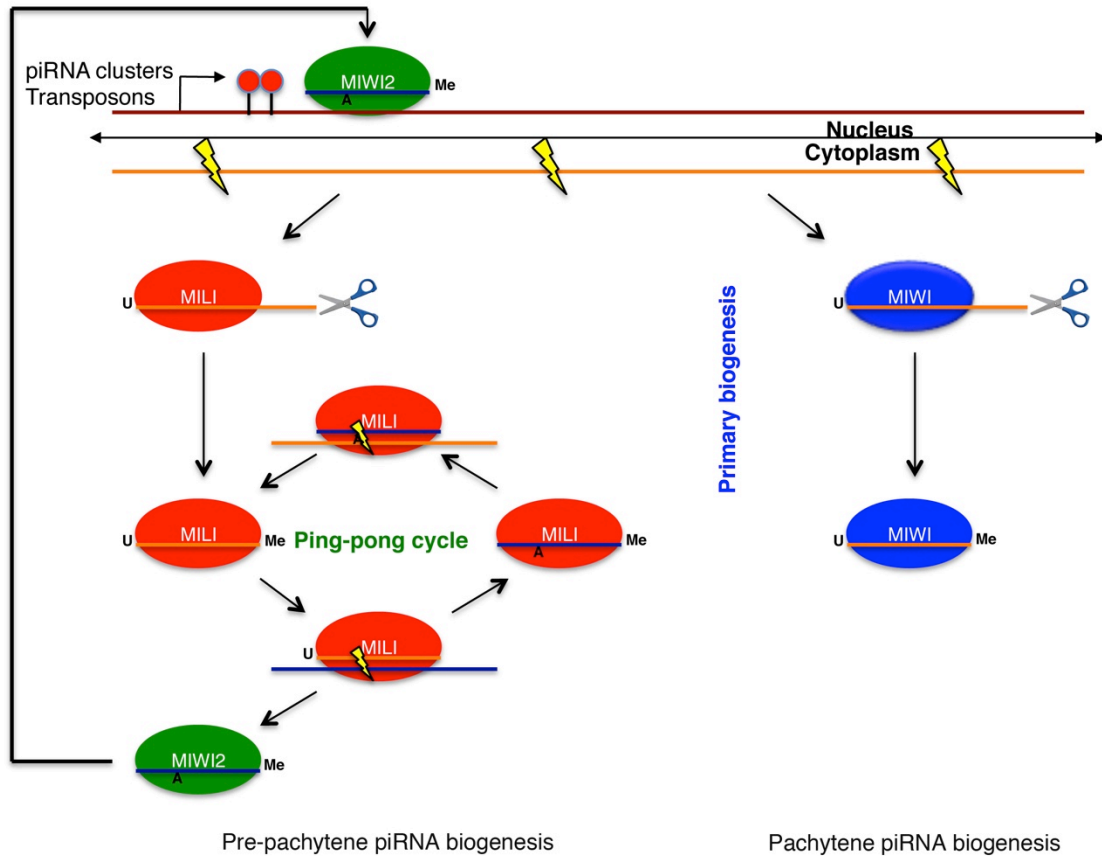
Figure 1.2: Framework for mammalian piRNA biogenesis. piRNA clusters are transcribed into piRNA precursor transcripts and are exported from the nucleus to the cytoplasm. During primary biogenesis, piRNA precursors are cleaved and incorporated into MILI and MIWI as piRNA intermediates. The 3' ends of piRNA intermediates are trimmed and methylated to generate piRNAs. During the ping-pong cycle, piRNAs guide MILI to cleave complementary RNAs to generate antisense secondary piRNAs, Secondary piRNAs loaded onto MILI guide MILI to cleave complementary RNAs to generate piRNAs with same sequence as the initial piRNA. Secondary piRNAs loaded onto MIWI2 guide MIWI2 into the nucleus to establish repressive methyl marks on active TEs. The red dots represent methyl marks on TEs. The yellow lighting bolts represent endonuclease activity. The scissors represent exonuclease activity. "U" signifies the bias for uridine residues at the 5' ends of piRNAs and piRNA intermediates. "Me" signifies the methylated 3' ends of piRNAs. "A" signifies the bias for adenine residues at the 10th position of secondary piRNAs.

المنارة للاستشارات

www.manaraa.com
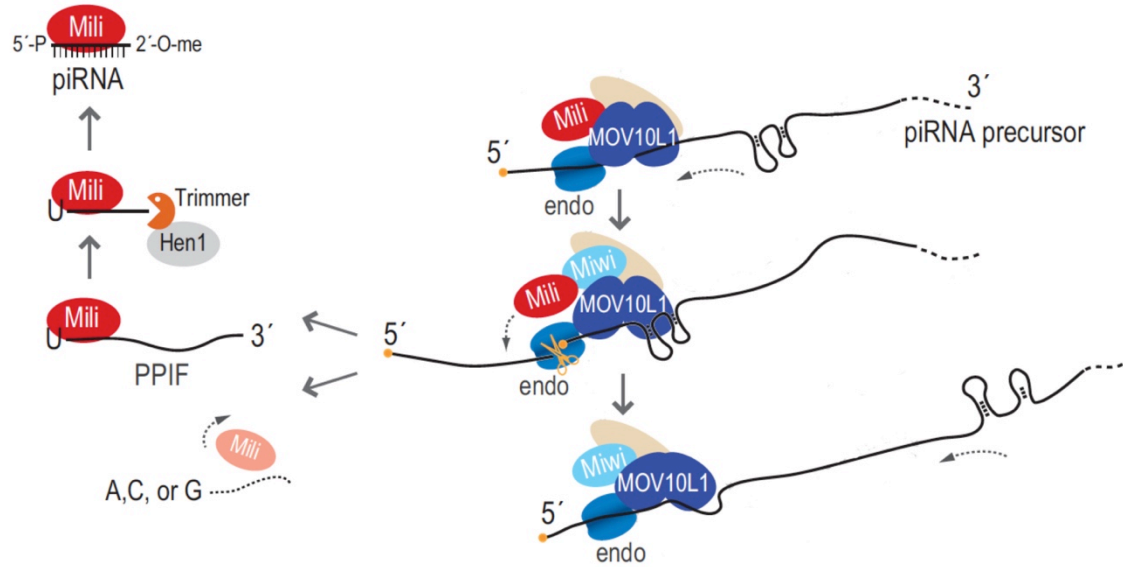
Figure 1.3: Proposed model for MOV10L1 function in piRNA biogenesis. MOV10L1 forms a complex with a Piwi protein, the endonuclease (MITOPLD), and additional factors (beige oval) required for primary biogenesis. MOV10L1 translocates along the piRNA precursor transcript in a 5′-to-3′ direction. MOV10L1 RNA helicase activity resolves secondary structures within the piRNA precursor and facilitates cleavage of the piRNA precursor by MITOPLD. piRNA precursor fragments are formed by two consecutive cleavage events. Piwi proteins preferentially incorporate piRNA precursor fragments containing 5' uridine residues. The Piwi protein and piRNA intermediate (PPIF) are released from the complex followed by 3′ end trimming and 2′-O methylation, resulting in mature piRNAs. This process repeats as MOV10L1 continues to translocate along the piRNA precursor.

22

CHAPTER 2. MATERIALS AND METHODS

Parts of this chapter were previously published in:

Vourekas A, Zheng K, **Fu Q**, Maragkakis M, Alexiou P, Ma J, Pillai RS, Mourelatos Z, Wang PJ. 2015. The RNA helicase MOV10L1 binds piRNA precursors to initiate piRNA processing. *Genes Dev* **29**:617–629.

Fu Q, Pandey RR, Leu A, Pillai RS, Wang PJ. 2016. Mutations in the MOV10L1 ATP hydrolysis motif cause piRNA biogenesis failure and male sterility in mice. *Biol Reprod.* pii: biolreprod.116.142430

MOV10L1 Protein Expression and Purification

The nucleotide sequence of MOV10L1 encoding the 1187 amino acids (Uniprot: Q99MV5) containing the mutation, K778A, was cloned into the pRK5 vector with an in-frame N-terminal Flag tag using Phanta Super-Fidelity DNA polymerase and ClonExpress II (Vazyme). The pRK5 constructs were used to transfect 293T cells with TurboFect transfection reagent (Thermo). 293T cells expressing mutant MOV10L1 were lysed by sonication in K150 lysis and immunoprecipitation buffer (50 mM HEPES at pH 7.5, 150 mM KoAc, 1 mM DTT, 0.1% NP-40 [Igepal] with EDTA-free protease inhibitors cocktail [Roche]), and the lysate was centrifuged at 16,000g for 20 min. The cleared lysate was mixed with 50 µL of M2 magnetic bead slurry (Sigma), prewashed with K150, and incubated for 2 h at 4°C. Immunoprecipitation beads were washed three times with K150, once with K150 containing 250 mM NaCl, and three more times with K150. The

beads were resuspended in 1 mL of K150 and kept on ice for a maximum of 2d. Fifty microliters of bead suspension contained 1 μg of mutant MOV10L1 protein.

RNA Duplex Unwinding Assay

The following RNA oligos were used: duplex with 5′ end overhang (Top 5′, 5′-GCGUCUUUACGGUGCU-3′ and Bottom 5′, 5′-AAAACAAAACAAAACAAAACAAAAUAGCACCGUAAAGACGC-3′) and duplex with 3′ end overhang (Top 3′, 5′-AGCACCGUAAAGACGC-3′, and Bottom 3′, 5′-GCGUCUUUACGGUGCUUAAAACAAAACAAAACAAAACAAAA-3′). The top oligos were 5′ end-labeled, and all four oligos were gel-purified. The duplexes were prepared in 50 mM MOPS (pH 6.5) and 5 mM EDTA. To detect the duplex-unwinding activity, 50 μL of MOV10L1-bound bead suspension (1 μg of MOV10L1 protein) was washed in reaction buffer (50 mM Tris at pH 7.5, 20 mM KoAc, 0.2 mM MgCl2, 0.01% Igepal [Nonidet P-40], 1 mM DTT); mixed with 20 nM duplex, 1 pmol of cold top oligo, and 20 U of rRNasin in 30 μL of reaction buffer; and incubated for 10 min at 37°C with shaking in a Thermomixer (1000 rpm). Subsequently, ATP was added at a final concentration 0.5 mM, and incubation was resumed for the indicated time. Four-microliter reaction samples were mixed with 4 μL of stop solution and kept on ice. Reaction products were analyzed by electrophoresis on a 12% acrylamide non-denaturing gel and visualized by autoradiography.

Generation of *Mov10l1* Knockin Alleles

To generate the *Mov10l1* knock-in targeting constructs, DNA fragments were amplified by high-fidelity PCR using a *Mov10l1* BAC clone (RP23-269F24). Codon 778 (exon 17) was mutated from AAG (lysine) to GCG (alanine) by PCR-based mutagenesis

to generate the *Mov10l1*-KI targeting construct. Codons 888 and 889 (exon 20) were mutated from GAC GAG (aspartic acid glutamic acid) to GCG GCG (alanine alanine) by PCR-based mutagenesis to generate the *Mov10l1*-KI2 targeting construct. The neomycin selection cassette was flanked by loxP sites for Cre-mediated removal. The targeting constructs were sequenced to confirm the mutations and linearized by digestion with *Cla*I. V6.5 hybrid ES cells were electroporated with linearized targeting constructs separately and cultured in the presence of 350 μg/mL G418. 392 G418-resistant ES cell clones were screened for homologous recombination of each construct. One targeted ES clone was obtained for the *Mov10l1*-KI allele and injected into blastocysts. Four targeted ES clones were obtained for the *Mov10l1*-KI2 allele, and one clone was injected into blastocysts. The *Mov10l1* knock-in alleles were transmitted through the germline. To delete the neo selection cassette, *Mov10l1*$^{KI/+}$ and *Mov10l1*$^{KI2/+}$ mice were crossed with *Actb*-Cre mice that express Cre ubiquitously (Lewandoski and Martin 1997). All of the studies were performed with mice without the neo cassette. The wild-type (439-base-pair [bp]) and *Mov10l1*-KI (557-bp) alleles were assayed by PCR with the primers ACCTCCGGGAACTGGAGCGACTGTG and ATCCCAAGCCCGGCTTGCAGTA. The wild-type (480-bp) and *Mov10l1*-KI2 (598-bp) alleles were assayed by PCR with primers GCCAGGTAAGGCCTGTGTCTT and GCCTAGTGACTGAAAGGAGGGA. PCR primers flanked the remaining loxP site and adjacent vector sequence. Schematics for the generation of the two *Mov10l1* knockin alleles are shown in Figure 2.1.

Mouse Breeding

Mice were housed in a barrier vivarium, monitored daily, and under veterinarian care by the attending veterinarians from University Laboratory Animal Resources

(ULAR) at the University of Pennsylvania. All experimental protocols were approved by the Institutional Animal Care and Use Committee (IACUC) of the University of Pennsylvania.

RNA Isolation, RT-PCR, and qRT-PCR

Total RNA was extracted from testes using Trizol reagent (Invitrogen), treated with DNase I (Invitrogen), and reverse transcribed to cDNA using M-MLV reverse transcriptase (Promega) according to the manufacturer's instructions. *Mov10l1* expression and *Actb* expression levels in 10-day old *Mov10l1* knockin mice were assayed by RT-PCR. Expression levels of pre-pachytene piRNA precursors were assayed by qRT-PCR using Prism (Applied Biosystems) Real-Time PCR Systems and Power SYBR Green reaction mix (Applied Biosystems 4367659). Relative expression levels were calculated using the ddCt method. We examined mapping locations of the embryonic day 18 MILI IP piRNAs identified by the Pillai group (Xiol et al., 2012) to identify areas of high pre-natal piRNA density, that constitute the pre-natal piRNA clusters. We designed pairs of primers to amplify three amplicons, and one more pair of primers was designed to detect Hist1h1a mRNA, which is also processed into piRNAs. Care was taken so that the above primers hybridize on unique sequences and not on repeat sequences. GAPDH was used as internal reference. Primers used for RT-PCR and qRT-PCR are listed in Table 2.1.

Immunoblot Analysis

Testes were homogenized in lysis buffer (100mM Tris pH 6.8, 2.5% SDS (w/v), 7.5% glycerol (v/v), 5% β-mercaptoethanol (v/v)). Lysates were reduced in sample buffer. Proteins were resolved by 8% SDS-PAGE and transferred to PVDF membranes

(Millipore). Membranes were blocked with 10% milk in TBST and incubated in primary antibody for 1 hr at room temperature (RT). After incubation with HRP secondary antibody (cell signaling) for 1 hour at RT, proteins were detected using ECL Western Blotting Detection Reagents (GE-Amersham Biosciences). Primary antibodies used are listed in Table 2.2.

Immunoprecipitation and Detection of piRNAs

Affinity purified anti-MILI (Reuter et al. 2011) and anti-MIWI2 (crude serum from rabbit) (Pandey et al. 2013) were bound to protein G–Sepharose 4 Fast Flow beads (GE healthcare) and used to purify MILI and MIWI2 complexes from embryonic mouse testis extracts (50 mM Tris, pH 8, 150 mM NaCl, 5 mM MgCl2, 10% glycerol, 1mM DTT, 0.5% sodium deoxycholate (Sigma), 1% Triton X-100, 1 tablet of complete protease inhibitor (Roche) per 5 ml, 2 mM Vanadyl ribonucleoside complex (Sigma)). Ten pairs of E16.5 testes of each genotype were homogenized for MILI and MIWI2 immunoprecipitation. After five washes (10 mM Tris, pH 8, 150 mM NaCl, 0.05% (v/v) NP-40), the retained proteins in RNA complexes were digested by proteinase K (42°C, 30 minutes) and finally associated RNA were isolated by phenol chloroform extraction and precipitated in ethanol. To visualize RNAs, they were de-phosphorylated with rAPid alkaline phosphatase (recombinant bovine phosphatase; Roche) and 5′-end labeled with γ-[32P]-ATP with T4 polynucleotide kinase (Thermo Scientific). The labeled RNAs were resolved by 15% (w/v) urea-PAGE. Gels were exposed to Phosphor Storage screens (GE Health) and scanned (Typhoon scanner; GE Health).

27

Histology

Testes were fixed in Bouin's solution overnight and dehydrated in a series of ethanol and xylene washes: 50% rinse (3x), 70% 1 hr. (2x), 95% 1 hr. (2x), 100% 1 hr. (2x), xylene 1.5 hr. (2x). Sections were embedded in paraffin, sectioned, and stained with hematoxylin and eosin.

Immunofluorescence

Immunofluorescence was performed on frozen sections of testes fixed in 4% paraformaldehyde at 4°C. Testes from embryonic and 6-week old mice were fixed for 3 hours and overnight, respectively. Sections were blocked for 1 hour at room temperature with a buffer containing 10% goat serum. Sections were then incubated with the primary antibody for 1 hour at 37°C. The blot was washed three times and incubated with a fluorescein secondary antibody (Vector Laboratories) (1:100 dilution) for 1 hour at 37°C. Sections were washed three times. DNA was stained with DAPI. Primary antibodies used for immunofluorescence are listed in Table2.2.

Small-RNA Sequencing and Bioinformatic Analysis

RNAs present in endogenous MILI from testes of E16.5 *Mov10l1*^KI2/KI2 were isolated. Briefly, immunoprecipitations were treated with Proteinase K in 300 µL reaction at 42°C for 15 min (10 mM Tris-HCl pH 7.5, 5 mM EDTA, 0.5% SDS). RNAs present in the sample were purified by phenol-chloroform extraction and precipitation with ethanol. Approximately 20% of the sample was radioactively labeled at the 5′ end and mixed with the cold RNA. This mixture of radiolabeled and cold RNA was resolved by 15% urea-PAGE, and the RNAs present in the region (~20-40 nt) was excised and placed in nuclease-free tube. The gel was crushed in the tube and 400 µl of 0.4 M NaCl was

added to it. The RNA was eluted from the gel overnight at 25°C in a thermomixer. Gel pieces were removed by filtering the RNA containing gel with SpinX column (Costar, cat. No. 8160). RNA was directly precipitated with glycogen (10-20 μg) and absolute ethanol (1.0 ml) at -20°C overnight. Next day, RNA samples were centrifuged at 16000 x g for 30 minutes. The pellet was washed once with 75% ethanol and finally dissolved in 6 μl RNase free water. RNA was directly used for library preparation. Libraries were prepared (barcoded at 3′ end) using NEBNext® Multiplex Small RNA Library Prep Set for Illumina® (NEB Catalogue No. E7300) following manufacture instructions. Libraries were sequenced with the Illumina HiSeq 2000 platform (EMBL GeneCore facilty) for 50 cycles. Bioinformatic Analysis was performed based on the methods described in Pandey et al.2013.

TABLES

Mov10l1 F	GGAAAGACTGTGACTATAATCGAGG
Mov10l1 R	CCTCACTCCATGGAAGATGAGAG
B-actin F	GCGTGACATCAAAGAGAAGCT
B-actin R	CTTGATCTTCATGGTGCTAGG
Amplicon1 F	ATGTCCACCACTTCTCCCAG
Amplicon1 R	TATGTGGGACCCTGACCTCT
Amplicon2 F	ACATTGGGCAGCAGATGTTG
Amplicon2 R	GGGACCAATGTGACGAGAGA
Amplicon3 F	AGCCAGAAGAAGCCAGGTAG
Amplicon3 R	CGTCGGTCTTTTGCTACTCG
Hist1h1a.1 F	GTCGCTCAGGCTGCTTCTAC
Hist1h1a.1 R	GGATGCTTTCGCCTTCACTGAC

Table 2.1: List of qRT-PCR primers used in the study.

Target	Antibody Company	Application(s)	Concentration(s)	References
MOV10 L1	Wang lab	Immunoblot/Immunofluorescence	1:500/1:5	Zheng et al. 2010
MILI	Pillai lab	Immunoblot	1:500	Reuter et al. 2009
MILI	Abcam	Immunofluorescence	1:100	
MIWI2	from J. Martinex and G. Hannon	Immunofluorescence	1:1000	Aravin et al. 2009
ORF1	from S.L. Martin and A. Bortvin	Immunofluorescence	1:1000	Zheng et al. 2010
GAG	from B.R. Cullen	Immunofluorescence	1:5000	Zheng et al. 2010
B-actin	Sigma-Aldrich	Immunoblot	1:20000	

Table 2.2: List of antibodies used in the study.

31
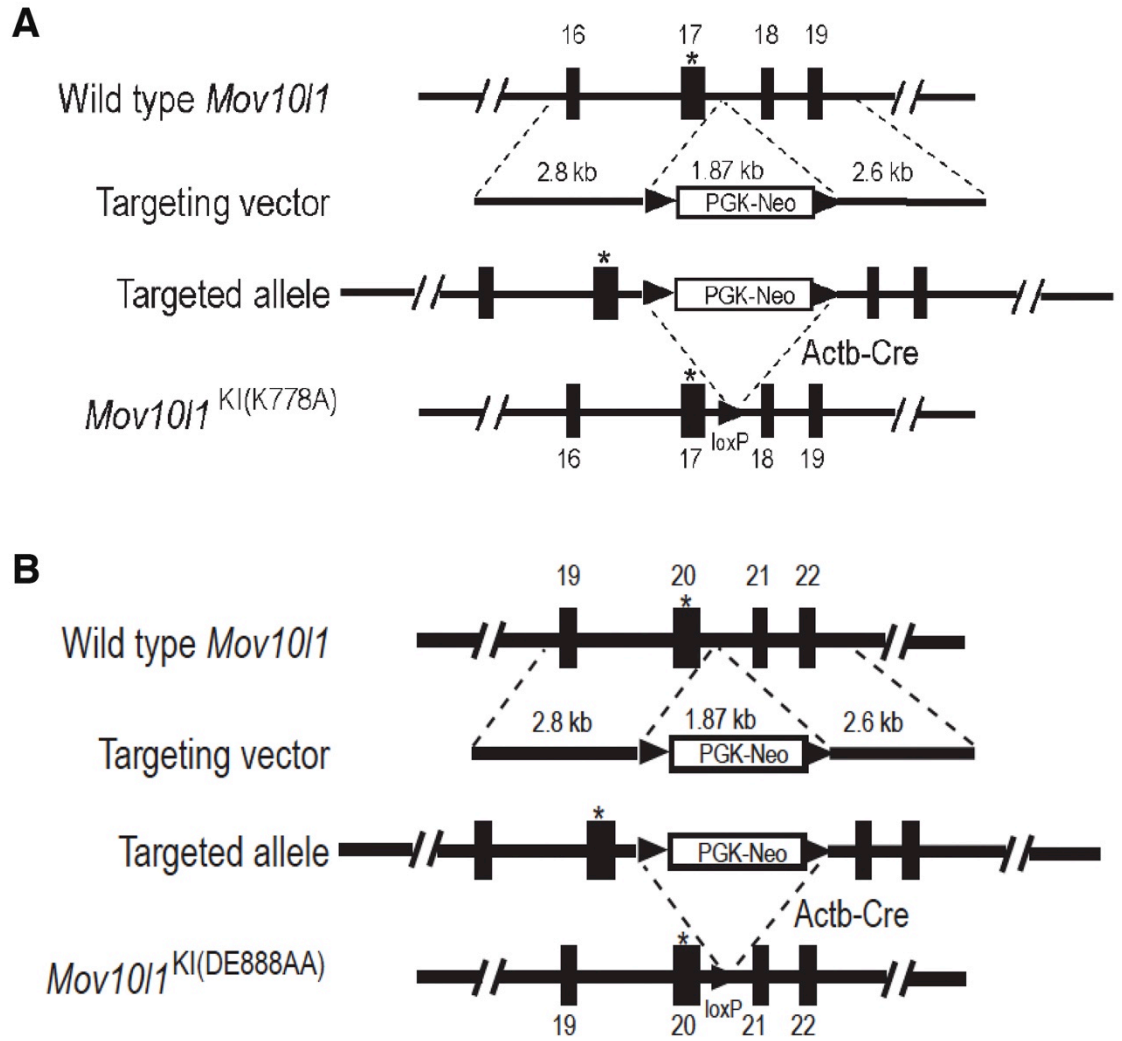
Figure 2.1: Generation of *Mov10l1* knockin alleles. **A)** Generation of the *Mov10l1*-KI allele. **B)** Generation of the *Mov10l1*-KI2 allele. The positions of the K→A **(A)** and DE→AA mutations **(B)** in *Mov10l1* are denoted by asterisks. The neo selection cassette is flanked with *loxP* sites and is removed by *Actb*-Cre.

CHAPTER 3. MOV10L1 ATP BINDING ACTIVITY IS REQUIRED FOR PIRNA BIOGENESIS

Parts of this chapter were previously published in:

Vourekas A, Zheng K, **Fu Q**, Maragkakis M, Alexiou P, Ma J, Pillai RS, Mourelatos Z, Wang PJ. 2015. The RNA helicase MOV10L1 binds piRNA precursors to initiate piRNA processing. *Genes Dev* **29**:617–629.

RESULTS

Generation of a *Mov10l1* knockin allele harboring a mutation in the ATP binding motif

Previous studies of MOV10L1 suggest MOV10L1 acts as an RNA helicase in the processing of piRNA precursors into mature piRNAs. In this chapter, we test the hypothesis that MOV10L1 RNA helicase activity is required for its role in piRNA biogenesis. MOV10L1 is a Superfamily I helicase (Fairman-Williams et al., 2010). The RNA helicase domain of MOV10L1 contains two Rec A-like domains (Figure 3.1A). The RNA helicase activities of Superfamily I helicases are dependent upon ATP binding and ATP hydrolysis (Tanner and Linder, 2001). To determine the requirement for MOV10L1 RNA helicase activity in piRNA biogenesis, we generated a *Mov10l1* knockin allele harboring a point mutation, K778A, in the ATP binding (Walker A) motif of the MOV10L1 RNA helicase domain (*Mov10l1*[KI]). The residue that was mutated is conserved among MOV10L1 and its homologs: UPF1 and ARMITAGE (Figure 3.1B). Mutation of the same residue in UPF1 abolished its RNA helicase activity (Weng et al., 1996). To determine whether mutation of the lysine residue in the *Mov10l1* ATP binding motif abolishes its

33

RNA helicase activity, we engineered a MOV10L1 Flag-tagged construct containing a mutation in the same lysine residue. We purified Flag-tagged protein from 293T cells transfected with the mutant MOV10L1 construct. The wildtype and mutant MOV10L1 proteins were expressed at similar levels in 293T cells (Figure 3.2A). Previous studies assayed for MOV10L1 RNA helicase activity using an RNA duplex unwinding assay (Vourekas et al., 2015). Using the same assay, we incubated purified mutant MOV10L1 protein with an RNA duplex containing a 5' overhang. The mutant MOV10L1 protein was not able to dissociate the RNA duplex (Figure 3.2B). This result shows that the lysine residue in the *Mov10l1* ATP binding motif is critical for its RNA helicase activity *in vitro*.

Mov10l1[KI/KI] males exhibit meiotic arrest and sterility

We crossed *Mov10l1*[KI/+] male and *Mov10l1*[KI/+] female mice to generate *Mov10l1*[KI/KI] mice. The heterozygous mice developed normally and were fertile, showing that the mutation is not dominant negative. *Mov10l1*[KI/KI] mice developed with no apparent defects. However, adult males and females were sexually dimorphic. The females were fertile while males were sterile. We examined germ cell development in adult male *Mov10l1*[KI/KI] mice. The testis sizes of 6-week old *Mov10l1*[KI/KI] mice were significantly smaller than their heterozygous counterparts (Figure 3.3A). We examined the histology of testes from 8-week old *Mov10l1* knockin mice by staining the testes with hematoxylin and eosin. There were no spermatogenic defects in the seminiferous tubules of *Mov10l1*[KI/+] mice (Figure 3.3B). However, spermatogenesis was arrested at the leptotene/zygotene stage of meiosis I in the seminiferous tubules of *Mov10l1*[KI/KI] mice (Figure 3.3B). This is supported by the lack of mature sperm in the caudal epididymis of these mice (data not shown). Thus, MOV10L1 ATP binding activity is required for meiosis and male fertility.

34

MILI is depleted of piRNAs in *Mov10l1*[KI/KI] embryonic germ cells

Meiotic arrest is associated with defects in pre-pachytene piRNA biogenesis in many piRNA pathway mutants (Table 1.1). To determine whether pre-pachytene piRNA biogenesis is impaired in *Mov10l1*[KI/KI] mice, we assayed for MILI-bound pre-pachytene piRNAs in testes from E16.5 *Mov10l1* knockin mice. Pre-pachtyene piRNAs are highly abundant at this timepoint (Aravin et al., 2008). We isolated MILI-bound RNAs from E16.5 *Mov10l1* knockin mice using RNA immunoprecipitation and detected piRNAs using UREA-PAGE. A beads sample in which no MILI antibody was added was used as a negative control. MILI-bound pre-pachytene piRNAs (26 nt) were present in the testes of E16.5 *Mov10l1*[KI/+] mice, but were absent in the testes of E16.5 *Mov10l1*[KI/KI] mice (Figure 3.4). Immunoblot analysis shows MILI was pulled down in testes from E16.5 *Mov10l1*[KI/+] and *Mov10l1*[KI/KI] mice, but not in the control sample (Figure 3.4). As expected, MILI-bound pre-pachytene piRNAs were also absent in the control sample (beads-only) (Figure 3.4). The depletion of MILI-bound pre-pachytene piRNAs in the testes of *Mov10l1*[KI/KI] mice shows that MOV10L1 ATP binding activity is required for the loading/biogenesis of piRNAs.

Accumulation of piRNA precursors in *Mov10l1*[KI/KI] embryonic testes

We then measured the expression of pre-pachytene piRNA precursors in the testes of E16.5 *Mov10l1* knockin mice to determine how the processing of piRNA precursors is affected in *Mov10l1*[KI/KI] mice. We used qRT-PCR to amplify regions of pre-pachytene piRNA precursor transcripts and *Hist1h1a*, an mRNA that is processed into piRNAs. Each amplicon denotes a region of a pre-pachytene piRNA precursor transcript or *Hist1h1a* containing a high density of piRNAs (Figure 3.5A). The expression levels of

35

the amplicons were significantly upregulated in the testes of *Mov10l1*^{KI/KI} mice compared to *Mov10l1*^{KI/+} mice (Figure 3.5B). The accumulation of piRNA precursors in the testes of *Mov10l1*^{KI/KI} mice shows MOV10L1 ATP binding activity is required for the processing of pre-pachytene piRNA precursors.

De-repression of LINE1 retrotransposons in *Mov10l1*^{KI/KI} embryonic germ cells

Pre-pachytene piRNA biogenesis is required to silence active LINE1 retrotransposons in gonocytes and spermatocytes. We decided to examine LINE1 activity in the testes of E16.5 *Mov10l1* knockin mice using immunofluorescent staining. We stained for ORF1, a protein that is encoded by the *Line1* transcript (Martin and Branciforte, 1993). ORF1 was barely detectable in the gonocytes of E16.5 *Mov10l1*^{KI/+} mice, but displayed very strong staining in the gonocytes of E16.5 *Mov10l1*^{KI/KI} mice (Figure 3.6). This result shows that LINE1 retrotransposons are highly de-repressed in the gonocytes of *Mov10l1*^{KI/KI} mice. Thus, MOV10L1 ATP binding activity is required to silence LINE1 retrotransposons in the germline.

Polar conglomeration of piRNA pathway proteins in *Mov10l1*^{KI/KI} embryonic germ cells

The loss of pre-pachytene piRNAs and de-repression of LINE1 retrotransposons in the testes of E16.5 *Mov10l1*^{KI/KI} mice shows that the piRNA pathway is impaired at this stage. We decided to examine how individual components of the piRNA pathway are affected in the *Mov10l1* ATP binding mutant. We analyzed MOV10L1 and MILI expression in testes from E16.5 *Mov10l1* knockin mice, using B-ACTIN as a control. The wildtype and mutant MOV10L1 proteins were expressed at similar levels in the testes of E16.5 *Mov10l1*^{KI/+} and *Mov10l1*^{KI/KI} mice (Figure 3.7). MILI was also expressed at similar

levels in the testes of E16.5 *Mov10l1*^{KI/+} and *Mov10l1*^{KI/KI} mice (Figure 3.7). Thus, mutation of *Mov10l1* ATP binding motif didn't affect its expression or the expression of other components of the piRNA pathway in gonocytes. The depletion of piRNAs can affect the localization of components of the piRNA pathway. MIWI2 is predominantly localized to the nucleus, but is excluded from the nucleus in the absence of piRNAs (Aravin et al., 2008). We examined the localization of MIWI2 in the testes of E16.5 *Mov10l1* knockin mice using immunofluorescent staining. As expected, MIWI2 was predominantly localized to the nucleus of gonocytes E16.5 *Mov10l1*^{KI/+} mice, but was excluded from the nucleus of gonocytes in E16.5 *Mov10l1*^{KI/KI} mice (Figure 3.8). Interestingly, MIWI2 also formed a polar granule in the cytoplasm of gonocytes in E16.5 *Mov10l1*^{KI/KI} mice (Figure 3.8). We then examined the localization of MOV10L1 and MILI in the testes of E16.5 *Mov10l1* knockin mice. In E16.5 *Mov10l1*^{KI/+} mice, MOV10L1 and MILI are diffusely localized throughout the cytoplasm of gonocytes (Figure 3.8). However, the mutant MOV10L1 protein and MILI also form a polar granule in the cytoplasm of gonocytes in E16.5 *Mov10l1*^{KI/KI} mice (Figure 3.8). The polar conglomeration of MOV10L1, MILI, and MIWI2 in the gonocytes of E16.5 *Mov10l1*^{KI/KI} mice shows that MOV10L1 ATP binding activity is required for the proper localization of components of the piRNA pathway.

DISCUSSION

In this chapter, we were able to determine the requirement for MOV10L1 ATP binding activity in piRNA biogenesis *in vivo* by characterizing the phenotype of a *Mov10l1* knockin mutant containing a mutation in the *Mov10l1* ATP binding motif. ATP binding is required for MOV10L1 RNA helicase activity. MOV10L1 protein containing a mutation in the ATP binding motif was catalytically inactive *in vitro*. The phenotypes

37

displayed by the *Mov10l1* ATP binding mutant show that MOV10L1 ATP binding activity is required for piRNA biogenesis. MILI-bound pre-pachytene piRNAs were depleted in the *Mov10l1* ATP binding mutant. MIWI2 was excluded from the nuclei of gonocytes and LINE1 retrotransposons were de-repressed in the gonocytes of embryonic *Mov10l1* ATP binding mutants. Adult *Mov10l1* ATP binding mutants exhibited meiotic arrest and male sterility. Together, these results support the requirement for MOV10L1 RNA helicase activity in piRNA biogenesis. Additionally, we found that the expression levels of pre-pachytene piRNA precursor transcripts were upregulated in the *Mov10l1* ATP binding mutant. The depletion of piRNAs and accumulation of piRNA precursors suggest that MOV10L1 RNA helicase activity is required for the processing of piRNA precursors into mature piRNAs.

Intriguingly, components of the piRNA pathway form a polar granule in the cytoplasm of gonocytes in the *Mov10l1* ATP binding mutant. The exact cause of this phenotype remains a mystery. The polar conglomeration of piRNA pathway proteins has been observed in some piRNA pathway mutants including *Ngn3cre;Mov10l1*fl/∆, *Ddx4*, and *Mitopld* mutants but not in other piRNA pathway mutants such as *Tdrd1* and *Mili* mutants (Chuma et al., 2006; Kuramochi-Miyagawa et al., 2010; Watanabe et al., 2011; Zheng and Wang, 2012). Thus, a lack of piRNA biogenesis is not responsible for the polar conglomeration of piRNA pathway proteins. In *Mitopld* and *Ngn3cre;Mov10l1*fl/∆ mutants, the polar conglomeration of piRNA pathway proteins is accompanied by the abnormal formation/disappearance of nuages and aggregation of mitochondria (Watanabe et al., 2011; Zheng and Wang, 2012). MOV10L1, MITOPLD, and DDX4 may play a role in nuage formation and mitochondrial localization in the cell that is independent of piRNA biogenesis. A number of components in the piRNA pathway

38

including MITOPLD, TDRKH, and PNLDC1 are localized to the mitochondrial membrane and could be required for mitochondrial localization in the cell (Izumi et al., 2016; Saxe et al., 2013; Watanabe et al., 2011). Furthermore, in the *Mitopld* mutant, the components of the piRNA pathway are shown to form a ring around the centrosome (Watanabe et al., 2011). The centrosome is the primary microtubule-organizing center. Microtubules may also play an important role in nuage assembly and mitochondrial localization. The interplay between the nuages, mitochondria, and microtubules remains to be elucidated.

39
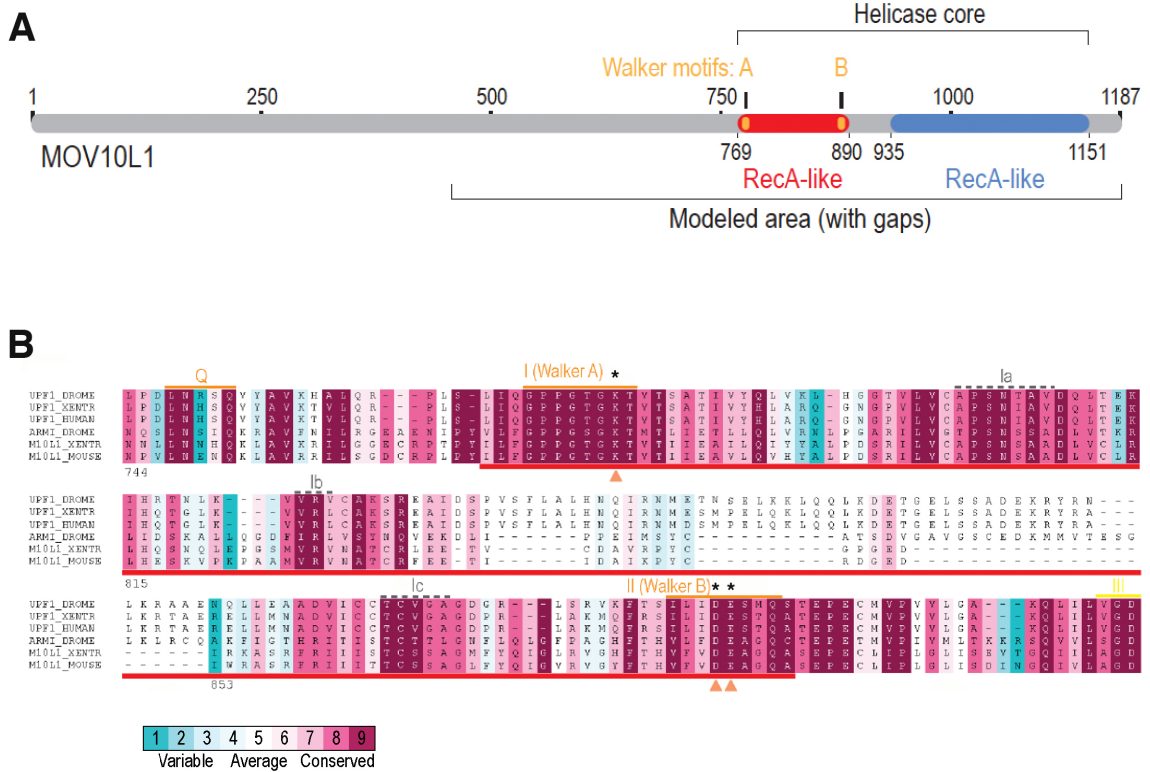
Figure 3.1: Mutation of conserved residues in the RNA helicase domain of MOV10L1. A) The RNA helicase domain of MOV10L1. The Walker A (ATP binding) and B (ATP hydrolysis) motifs are located in the first RecA-like helicase domain. **B)** Multiple sequence alignment of UPF1 and MOV10L1 homologues. The sequences of UPF1 and its homologs in human, *Xenopus tropicalis* (XENTR) and *D. melanogaster* (DROME), and MOV10L1 (M10L1) homologs in mouse, XENTR, and *D. melanogaster* (ARMI) are shown. The red line marks the first Rec-A like helicase domain. The conserved ATP binding (Walker A) and ATP hydrolysis (Walker B) motifs are marked with orange lines. Amino acid residues required for ATP binding and ATP hydrolysis in UPF1 are marked with orange triangles (Weng et al. 1996). Asterisks denote the mutation of these conserved residues to Alanines to generate the two *Mov10l1* knockin mouse models. Residues are highlighted with a color scheme according to conservation.
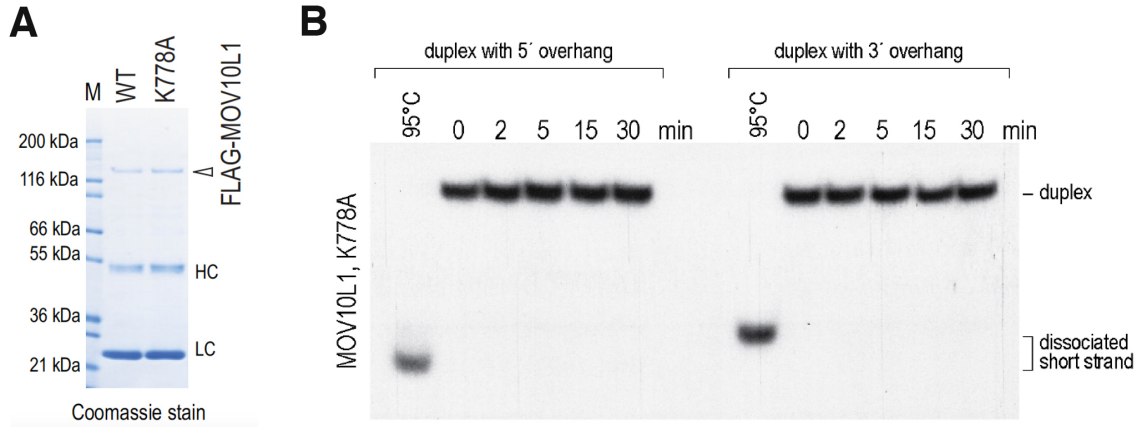
Figure 3.2: The MOV10L1 K778A protein is catalytically inactive. A) Purification of MOV10L1 wildtype (WT) and mutant (K778A) proteins from 293T cells. **B)** *In vitro* RNA duplex unwinding assay using purified MOV10L1 K778A protein.
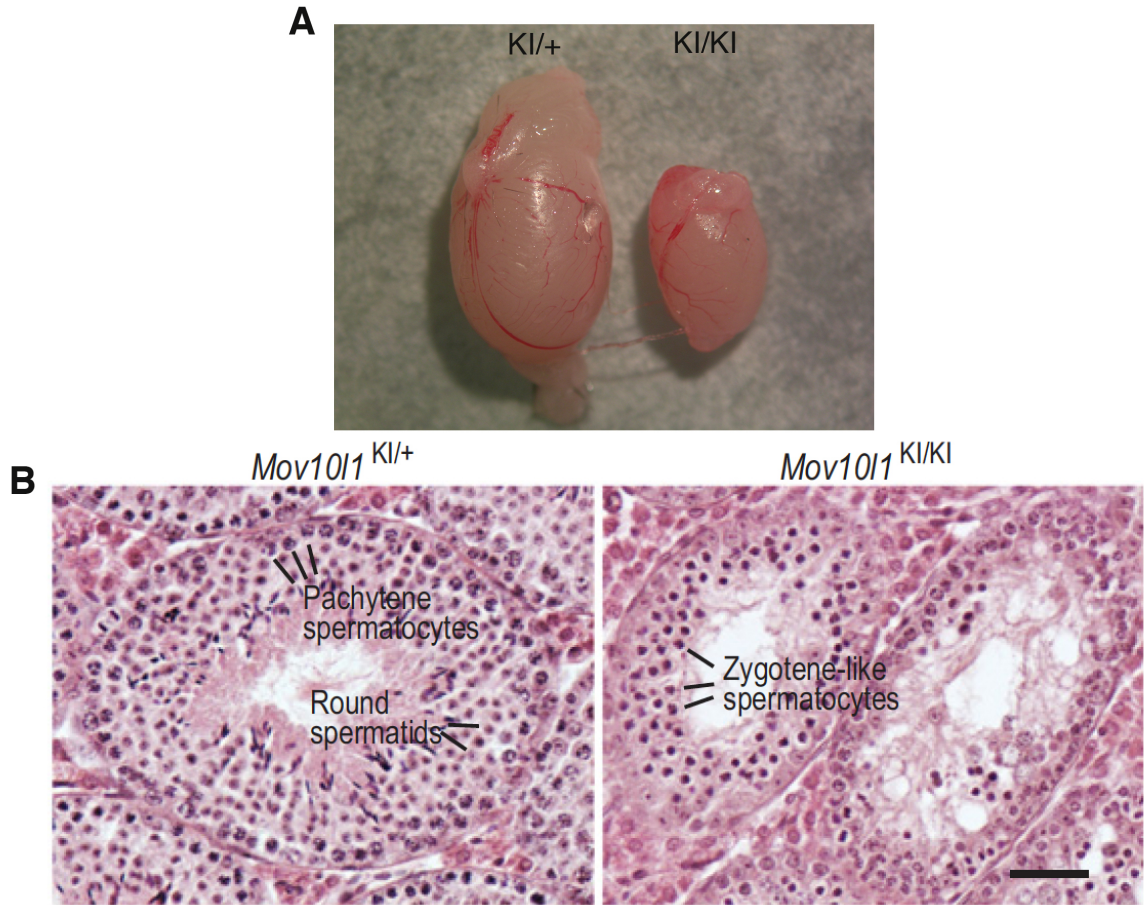
Figure 3.3: Adult *Mov10l1*^{KI/KI} males exhibit meiotic arrest. A) Dramatic size reduction of testes from 6-week old *Mov10l1*^{KI/KI} mice. **B)** Histology of testes from 8-week-old *Mov10l1*^{KI/+} and *Mov10l1*^{KI/KI} mice. Bars, 50 μm.
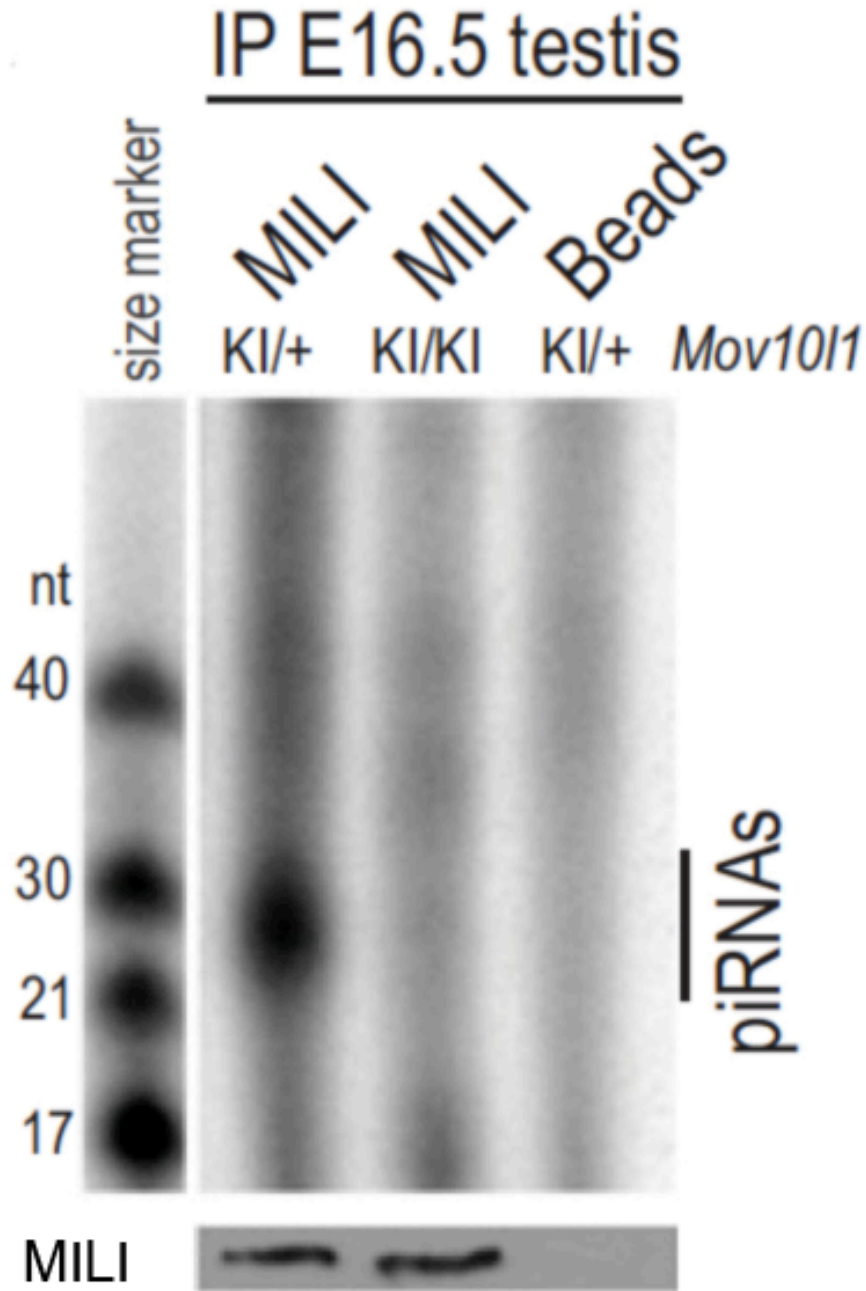
Figure 3.4: MILI is depleted of pre-pachytene piRNAs in embryonic *Mov10l1*[KI/KI] testes. The MILI complex was immunoprecipitated from the testes of E16.5 *Mov10l1*[KI/+] and *Mov10l1*[KI/KI] embryonic mice. 90% of the sample was used for analysis of RNAs isolated from MILI complexes. MILI-bound RNAs were radiolabeled for the detection of piRNAs (indicated by vertical line). 10% of the sample was used for detection of MILI by immunoblot analysis. Lysate incubated with uncoupled beads serves as a control.

43
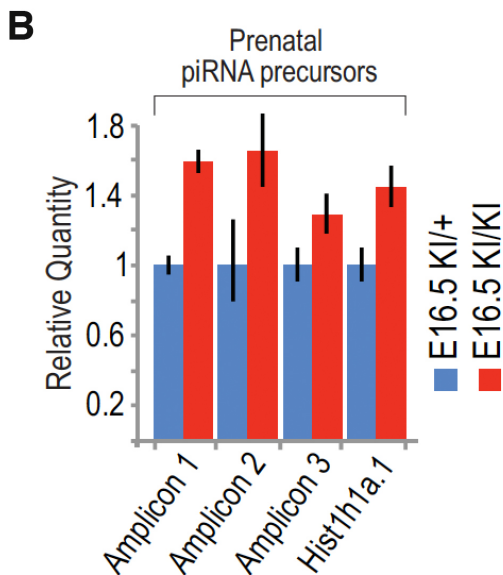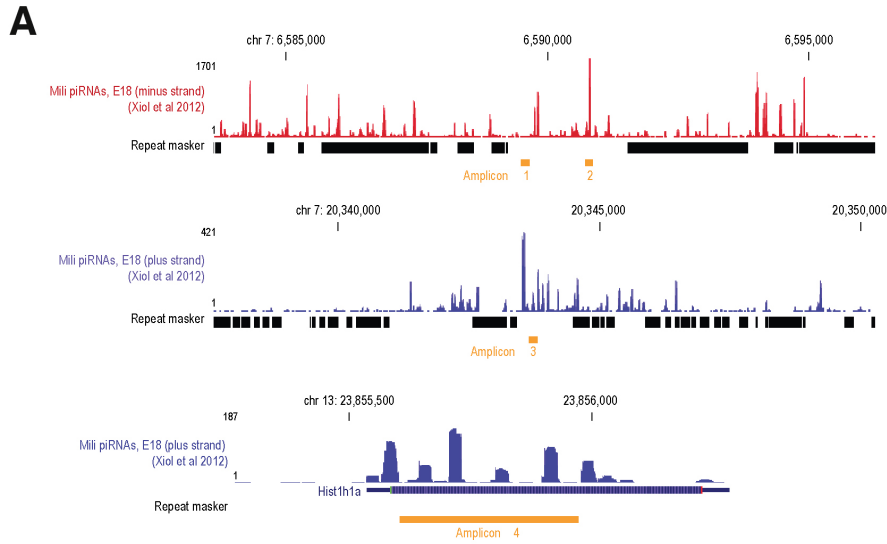
Figure 3.5: piRNA precursor expression levels are upregulated in embryonic _Mov10l1_[KI/KI] testes. A) Genome browser snapshots (mm9), showing pre-natal MILI-bound piRNAs at E18 (Xiol et al., 2012). The yellow bars denote the genomic positions of the four amplicons. **B)** Expression levels of amplicons in the testes of E16.5 _Mov10l1_[KI/+] and _Mov10l1_[KI/KI] mice.
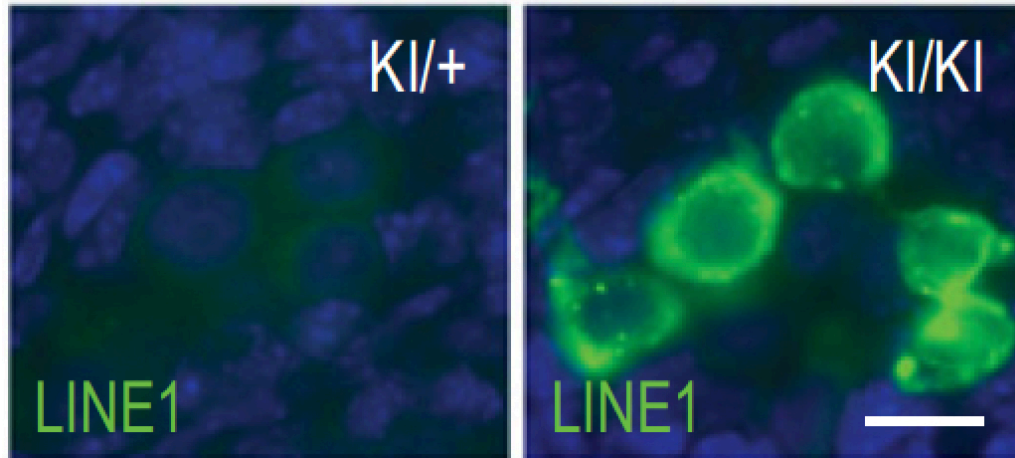
Figure 3.6: LINE1 retrotransposons are highly de-repressed in embryonic *Mov10l1*^{KI/KI} **gonocytes.** Sections of testes from E16.5 *Mov10l1*^{KI/+} and *Mov10l1*^{KI/KI} embryos were immunostained with antibodies against LINE1 ORF1 (Green). DNA was stained with DAPI (blue). Bar, 50 μm.
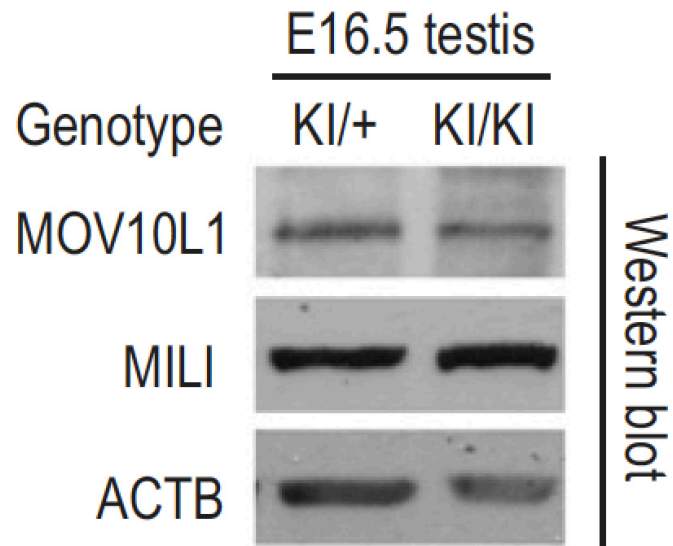
Figure 3.7: Expression of MOV10L1 and MILI in embryonic *Mov10l1* knockin testes. Detection of MOV10L1 and MILI in the testes of E16.5 *Mov10l1*[KI/+] and *Mov10l1*[KI/KI] mice using immunoblot analysis. B-actin was used as a control.
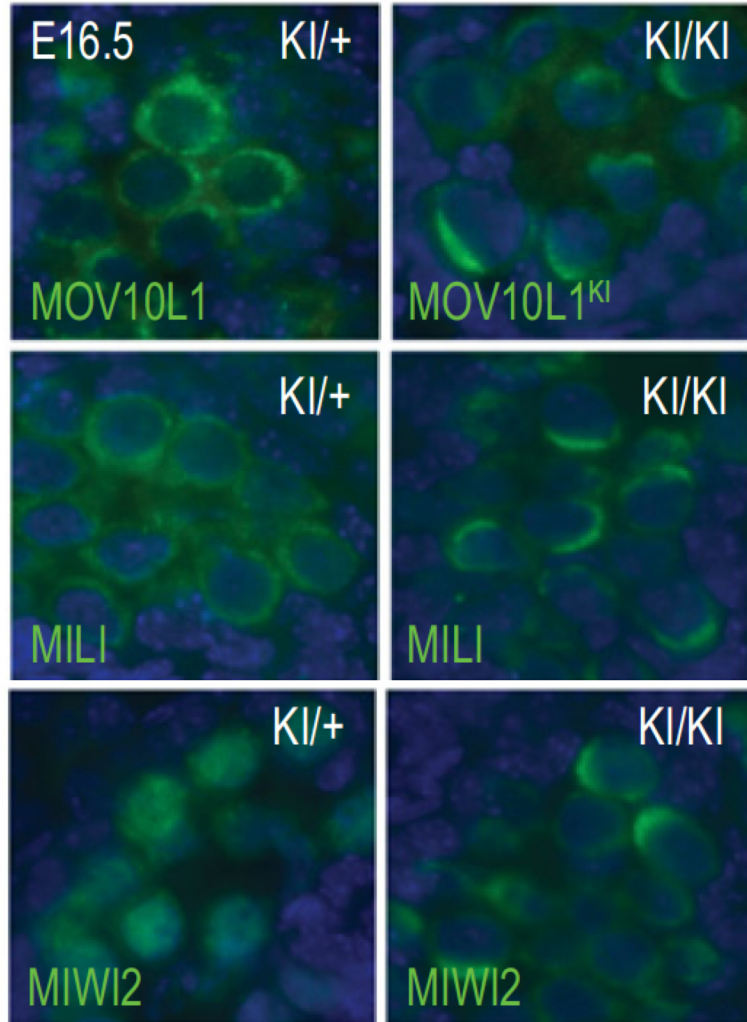
Figure 3.8: Polar conglomeration of piRNA pathway proteins in embryonic
Mov10l1[KI/KI] **gonocytes.** Sections of testes from E16.5 *Mov10l1*[KI/+] and *Mov10l1*[KI/KI]
embryos were immunostained with antibodies against MOV10L1, MILI, and MIWI2
(Green). DNA was stained with DAPI (blue). Bar, 50 μm.

CHAPTER 4: MOV10L1 ATP HYDROLYSIS ACTIVITY IS REQUIRED FOR PIRNA BIOGENESIS

Parts of this chapter were previously published in:

Fu Q, Pandey RR, Leu A, Pillai RS, Wang PJ. 2016. Mutations in the MOV10L1 ATP hydrolysis motif cause piRNA biogenesis failure and male sterility in mice. *Biol Reprod.* pii: biolreprod.116.142430

RESULTS
Generation of a *Mov10l1* knockin allele harboring a mutation in the ATP hydrolysis motif

In the previous chapter, we defined a requirement for MOV10L1 ATP binding activity in piRNA biogenesis using a knockin mouse model containing a point mutation in the *Mov10l1* ATP binding motif. UPF1 is one of the closest homologs of MOV10L1 (Vourekas et al., 2015). While UPF1 displays RNA helicase activity *in vitro*, UPF1 also displays activities that are dependent on ATP binding but not ATP hydrolysis. ATP binding to UPF1, independent of ATP hydrolysis, promoted dissociation of the UPF1:RNA complex *in vitro* (Weng et al., 1998). DEAD helicases, another family of RNA helicases, unwind RNA duplexes in a manner that is dependent on ATP binding but not ATP hydrolysis (Jankowsky, 2011). Furthermore, while MOV10L1 displays RNA helicase activity *in vitro*, this doesn't necessarily imply that it acts as an RNA helicase *in vivo.* Therefore, it is possible that MOV10L1 ATP binding activity is sufficient for piRNA biogenesis. To determine the requirement for MOV10L1 ATP hydrolysis activity in piRNA biogenesis *in vivo*, we generated a knockin allele containing a double point mutation

48

DE888AA in the *Mov10l1* ATP hydrolysis motif (*Mov10l1*^{KI2}). The residues that were mutated are conserved among MOV10L1, UPF1, and ARMITAGE (**Figure 3.1B**). Mutation of the same residues in UPF1 abolished its RNA helicase activity (Weng et al., 1996).

Adult *Mov10l1*^{KI2/KI2} males exhibit meiotic arrest and sterility

We crossed *Mov10l1*^{KI2/+} male and *Mov10l1*^{KI2/+} female mice to generate *Mov10l1*^{KI2/KI2} mice. The heterozygous mice were fertile, showing the mutation is not dominant negative. *Mov10l1*^{KI2/KI2} mice developed with no apparent defects. However, like the *Mov10l1* ATP binding mutant, adult *Mov10l1*^{KI2/KI2} males and females were sexually dimorphic. The females were fertile while males were sterile. We examined germ cell development in male *Mov10l1* knockin mice. The testis size of 6-week old *Mov10l1*^{KI2/KI2} mice (58 ± 5 mg) were significantly smaller than their heterozygous counterparts (155 ± 14 mg) (P = 0.001, Student's t-test) (Figure 4.1A) while the body weight of 6-week-old *Mov10l1*^{KI2/KI2} mice (21 ± 0.9 g) was similar to that of their heterozygous littermates (22.21 ± 1.9 g) (P = 0.1, Student's t-test). We then examined the histology of testes from 8-week old *Mov10l1* knockin mice by H&E staining. There were no spermatogenic defects in the seminiferous tubules of 8-week old *Mov10l1*^{KI2/+} mice (Figure 4.1B). In contrast, spermatogenesis was arrested at the leptotene/zygotene stage of meiosis I in the seminiferous tubules of 8-week old *Mov10l1*^{KI2/KI2} mice (Figure 4.1C). Thus, MOV10L1 ATP hydrolysis activity is required for meiosis and male fertility.

MILI and MIWI2 are depleted of piRNAs in *Mov10l1*^{KI2/KI2} embryonic germ cells

To determine whether pre-pachytene piRNA biogenesis is impaired in *Mov10l1*^{KI2/KI2} mice, we assayed for MILI-bound and MIW2-bound pre-pachytene piRNAs

49

in testes from E16.5 *Mov10l1* knockin mice using the same methods as described in the previous chapter. A beads sample in which neither MILI nor MIWI2 antibody was added served as a negative control. MILI-bound (26nt) and MIW2-bound piRNAs (28 nt) were present in the testes of E16.5 *Mov10l1*$^{KI2/+}$ mice, but were absent in the testes of E16.5 *Mov10l1*$^{KI2/KI2}$ mice (Figure 4.2). piRNAs were also absent in the control sample (Figure 4.2). The depletion of MILI- and MIWI2-bound pre-pachytene piRNAs in *Mov10l1*$^{KI2/KI2}$ mice shows MOV10L1 ATP hydrolysis activity is required for the loading/biogenesis of piRNAs. Interestingly, we also observed the presence of other MILI-associated small RNAs that were 20-40nt long in the testes of E16.5 *Mov10l1*$^{KI2/KI2}$ mice (Figure 4.2). Deep sequencing of the small RNAs suggests they are random sequences (data not shown). These small RNAs may be non-specific targets that were able to associate with MILI in the absence of piRNAs after cell lysis.

De-repression of LINE1 and IAP retrotransposons in *Mov10l1*$^{KI2/KI2}$ embryonic and post-natal germ cells

We then examined LINE1 and IAP activity in the testes of E16.5 and 6-week old *Mov10l1* knockin mice using immunofluorescent staining. We assayed for IAP activity by staining for GAG, a protein encoded by the *Iap* transcript. ORF1 was barely detectable in gonocytes of E16.5 *Mov10l1*$^{KI2/+}$ mice, but displayed very strong staining in the gonocytes of E16.5 *Mov10l1*$^{KI2/KI2}$ mice (Figure 4.3, C and D). GAG also displayed stronger staining in the gonocytes of E16.5 *Mov10l1*$^{KI2/KI2}$ mice compared to E16.5 *Mov10l1*$^{KI2/+}$ mice, although the increase in GAG staining was not as dramatic as the increase in ORF1 staining (Figure 4.3, A and B). ORF1 and GAG were also barely detectable in the germ cells of 6-week old *Mov10l1*$^{KI2/+}$ mice (Figure 4.4, A and C). In contrast, ORF1 displayed strong staining in the spermatocytes, and GAG displayed

50

strong staining in the spermatogonia of 6-week old *Mov10l1*^{KI2/KI2} mice (Figure 4.4, B and D). The increased staining of ORF1 and GAG in the embryonic and post-natal germ cells of *Mov10l1*^{KI2/KI2} mice shows LINE1 and IAP retrotransposable elements are de-repressed in the *Mov10l1* ATP hydrolysis mutant. Thus, MOV10L1 ATP hydrolysis activity is required for the silencing of retrotransposons in the germline.

Absence of mutant MOV10L1 protein in *Mov10l1*^{KI/KI} and *Mov10l1*^{KI2/KI2} post natal germ cells

We examined how individual components of the piRNA pathway are affected in the *Mov10l1* ATP hydrolysis mutant, focusing on the three proteins MOV10L1, MILI, and MIWI2. We used immunblot analysis to examine MOV10L1 and MILI expression in testes from not only embryonic but also post-natal *Mov10l1* knockin mice of different ages, using β-actin as a control. MOV10L1 and MILI were expressed in the testes of *Mov10l1*^{KI2/+} mice at all ages (Figure 4.5A). The mutant MOV10L1 protein was also expressed in the testes of E16.5 *Mov10l1*^{KI2/KI2} mice, albeit its expression was slightly reduced compared to the expression of wildtype MOV10L1 protein in E16.5 *Mov10l1*^{KI2/+} mice (Figure 4.5A). Surprisingly, the mutant MOV10L1 protein was not expressed in the testes of post-natal *Mov10l1*^{KI2/KI2} mice (Figure 4.5A). We measured *Mov10l1* mRNA levels in the testes of 10-day old *Mov10l1* knockin mice. *Mov10l1* mRNA levels were similar in 10-day old *Mov10l1*^{KI2/+} and *Mov10l1*^{KI2/KI2} mice (Figure 4.5B). MILI expression was also reduced in the testes of post-natal *Mov10l1*^{KI2/KI2} mice. We then examined the expression of MOV10L1 and MILI in testes from post-natal *Mov10l1* ATP binding mutants and their heterozygous counterparts, using β-actin as a control. Similarly, the

51

mutant MOV10L1 protein was not expressed, and MILI was reduced in testes of 10-day old *Mov10l1*[KI/KI] mice (Figure 4.5C).

Polar conglomeration of piRNA pathway proteins in *Mov10l1*[KI2/KI2] embryonic germ cells

Using immunofluorescent staining, we examined the localization of MOV10L1, MILI, and MIWI2 in the testes of E16.5 *Mov10l1* knockin mice. In E16.5 *Mov10l1*[KI2/+] mice, MOV10L1 and MILI are diffusely localized throughout the cytoplasm of gonocytes, while MIWI2 is predominantly localized to the nucleus of gonocytes (Figure 4.6, A, C, and E). In E16.5 *Mov10l1*[KI2/KI2] mice, all three piRNA pathway proteins form a polar granule in the cytoplasm of gonocytes (Figure 4.6, B, D, and F). MIWI2 was also excluded from the nucleus of gonocytes in E16.5 *Mov10l1*[KI2/KI2] mice (Figure 4.6B). The polar conglomeration of piRNA pathway proteins in the gonocytes of E16.5 and *Mov10l1*[KI2/KI2] mice shows MOV10L1 ATP hydrolysis activity is required for the proper localization of components of the piRNA pathway.

DISCUSSION

In this chapter, we were able to determine the requirement for MOV10L1 ATP hydrolysis activity in piRNA biogenesis *in vivo* by characterizing the phenotype of a *Mov10l1* mutant containing a mutation in the *Mov10l1* ATP hydrolysis motif. The *Mov10l1* ATP hydrolysis mutant displayed many of the same phenotypes as the *Mov10l1* ATP binding mutant we generated in the previous chapter. Both *Mov10l1* mutants exhibited a depletion of piRNAs associated with Piwi proteins, de-repression of retrotransposable elements, mislocalization of piRNA pathway proteins, meiotic arrest, and male sterility. Although we did not measure the expression levels of piRNA

52

precursors in the *Mov10l1* ATP hydrolysis mutant, we expect that they are also upregulated. The phenotypes displayed by the *Mov10l1* ATP hydrolysis mutant show that MOV10L1 ATP hydrolysis activity is required for piRNA biogenesis and that MOV10L1 ATP binding activity is not sufficient for piRNA biogenesis. Therefore, the requirement for both MOV10L1 ATP binding activity and MOV10L1 ATP hydrolysis activity in piRNA biogenesis *in vivo* shows MOV10L1 RNA helicase activity is required for piRNA biogenesis and the processing of piRNA precursors.

Interestingly, the mutant MOV10L1 proteins were not expressed post-natally in both the *Mov10l1* ATP binding mutant and *Mov10l1* ATP hydrolysis mutant. The absence of mutant MOV10L1 protein expression in the *Mov10l1* mutants post-natally is likely due to reduced protein stability as the mutant *Mov10l1* transcript levels were normal in the *Mov10l1* ATP hydrolysis mutant. It is possible that the residues that were mutated in the two *Mov10l1* mutants are critical for MOV10L1 stability. The absence of mutant MOV10L1 protein correlates with a reduction in MILI expression. MOV10L1 directly interacts with MILI. The stability of MILI may depend on the interaction of the two proteins.

We are not able to characterize the role of MOV10L1 RNA helicase activity in pachytene piRNA biogenesis using the *Mov10l1* ATP binding and *Mov10l1* ATP hydrolysis mutants due to meiotic arrest occurring in the knockin mutants before pachytene piRNAs are generated. To characterize the role of MOV10L1 RNA helicase activity in pachytene piRNA biogenesis, we generated trans-heterozygous *Mov10l1* mutants containing a *Mov10l1*-floxed allele and a *Mov10l1*-knockin allele. Expression of the *Mov10l1*-floxed allele was under the control of an Ngn3-Cre. Therefore, pre-pachytene piRNA biogenesis would not be affected in the trans-heterozygous *Mov10l1* mutants since wildtype MOV10L1 protein would be expressed in the mutants until the

leptotene/zygotene stage of meiosis. Like *Ngn3cre;Mov10l1*^{fl/Δ} mice, adult male

Ngn3cre;Mov10l1^{KI/FL} and *Ngn3cre;Mov10l1*^{KI2/FL} mice exhibited round spermatid arrest

(Figure 4.7, A-C). However, the mutant MOV10L1 proteins translated from the knockin

alleles were not expressed post-natally in *Ngn3cre;Mov10l1*^{KI/FL} and

Ngn3cre;Mov10l1^{KI2/FL} mice (Figure 4.7D). This was not too surprising since the mutant

proteins were also not expressed post-natally in *Mov10l1*^{KI/KI} and *Mov10l1*^{KI2/KI2} mice. Due

to the lack of mutant MOV10L1 protein expression, *Ngn3cre;Mov10l1*^{KI/FL} and

Ngn3cre;Mov10l1^{KI2/FL} mice could not be used to study the role of MOV10L1 RNA

helicase activity in pachytene piRNA biogenesis. Even so, multiple lines of evidence

point to a requirement for MOV10L1 RNA helicase activity in pachytene piRNA

biogenesis including the accumulation of pachytene piRNA precursors in post-natal

Mov10l1 mutants and the direct binding of MOV10L1 to pachytene piRNA precursors

(Vourekas et al., 2015; Zheng and Wang, 2012).

54
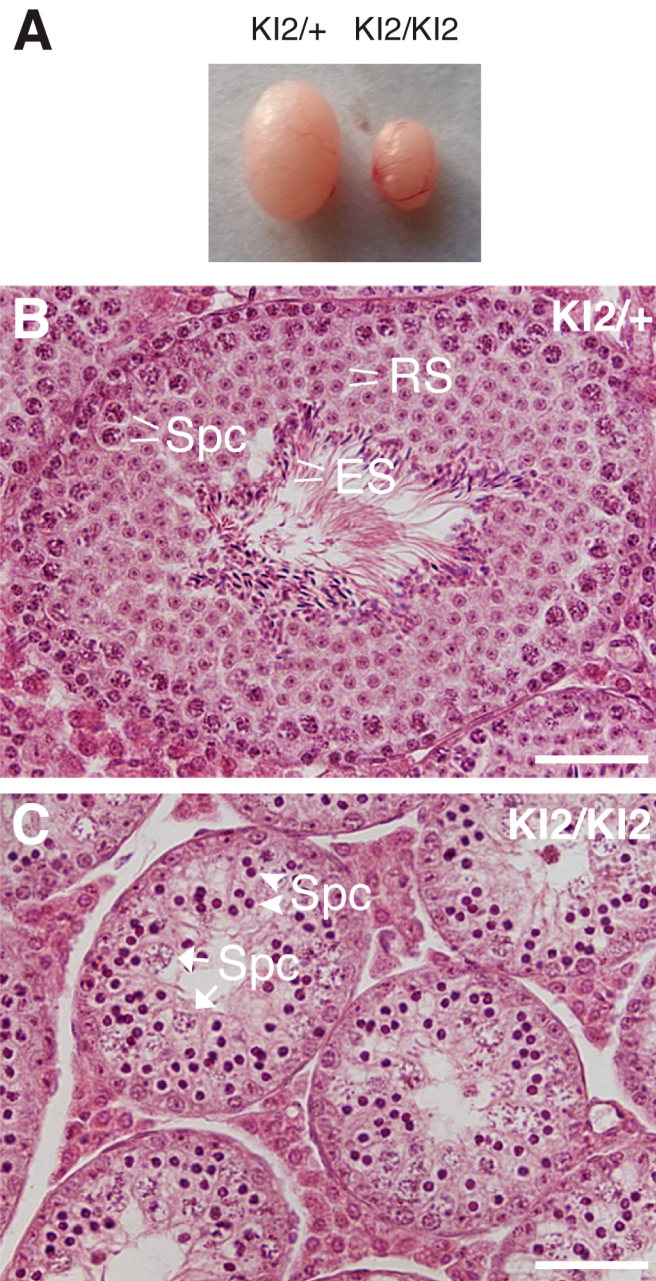
Figure 4.1: Adult *Mov10l1*^{KI2/KI2} males exhibit meiotic arrest. A) Dramatic size reduction of testis from 6-week-old *Mov10l1*^{KI2/KI2} mice. Histology of testes from 8-week-old *Mov10l1*^{KI2/+} **(B)** and *Mov10l1*^{KI2/KI2} **(C)** mice. Two types of spermatocytes with condensed nuclei (arrowheads) and enlarged nuclei (arrows) are present in the *Mov10l1*^{KI2/KI2} seminiferous tubules. Spc, spermatocytes; RS, round spermatids; ES, elongating spermatids. Bars, 50 μm.
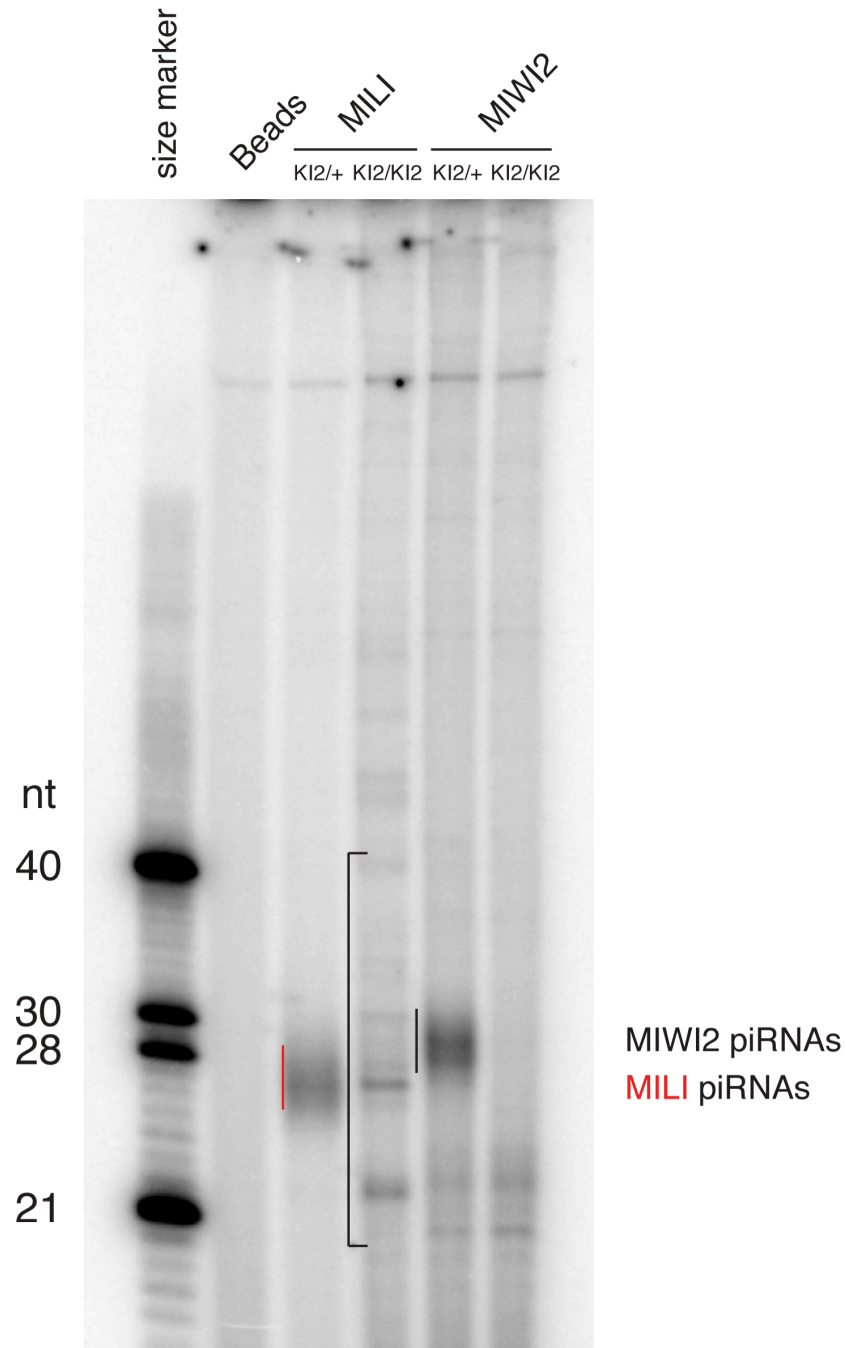
Figure 4.2: MILI and MIWI2 are depleted of pre-pachytene piRNAs in embryonic *Mov10l1*^KI2/KI2 testes. The MILI and MIWI2 complexes were immunoprecipitated from the testes of E16.5 *Mov10l1*^KI2/+ and *Mov10l1*^KI2/KI2 embryos. MILI-bound and MIWI2-bound RNAs were isolated from MILI and MIWI2 complexes and radiolabeled for the detection of piRNAs (indicated by red and black lines). Lysate incubated with uncoupled beads serves as a control. The RNAs (20 to 40 nt) (indicated by bracket) associated with MILI in the *Mov10l1*^KI2/KI2 testes were subjected to deep sequencing.

56
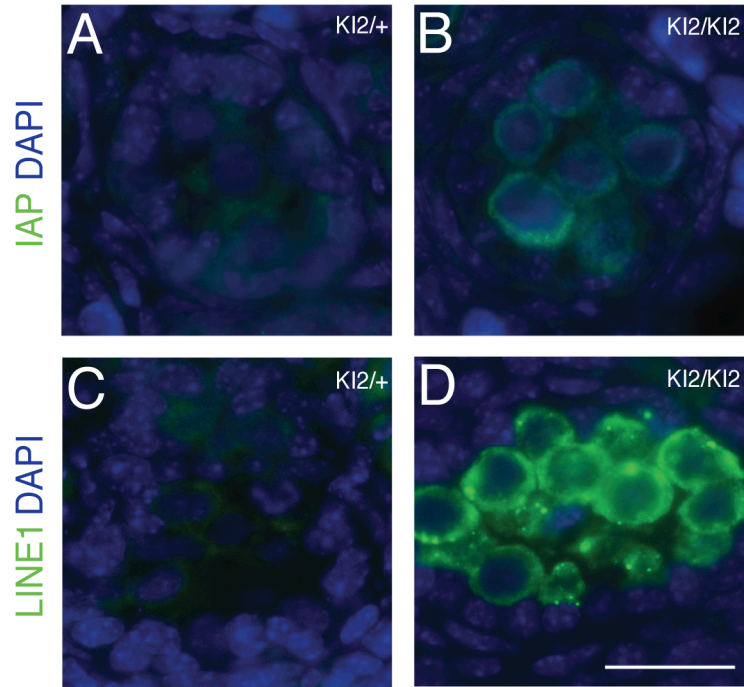
Figure 4.3: The LINE1 and IAP retrotranposons are de-repressed in embryonic _Mov10l1_^{KI2/KI2} gonocytes. Sections of testes from E16.5 _Mov10l1_^{KI2/+} and _Mov10l1_^{KI2/KI2} embryos were immunostained with antibodies against **(A and B)** IAP GAG and **(C and D)** LINE1 ORF1. DNA was stained with DAPI. Bar, 50 µm.
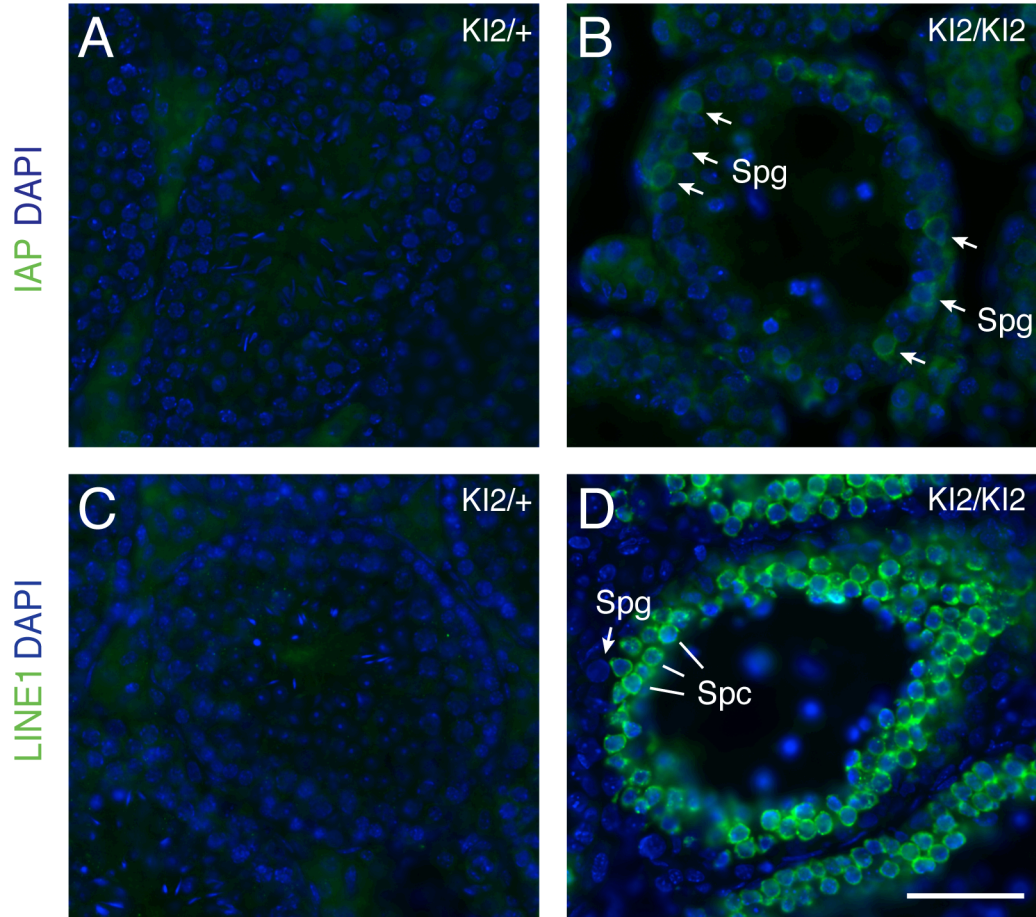
Figure 4.4: The LINE1 and IAP retrotransposons exhibit binary de-repression in post-natal _Mov10l1_^{KI2/KI2} testes. Sections of testes from 6-week-old _Mov10l1_^{KI2/+} and _Mov10l1_^{KI2/KI2} mice were immunostained with antibodies against **(A and B)** IAP GAG and **(C and D)** LINE1 ORF1. DNA was stained with DAPI. Spg, spermatogonia; Spc, spermatocytes; Bar, 50 µm.
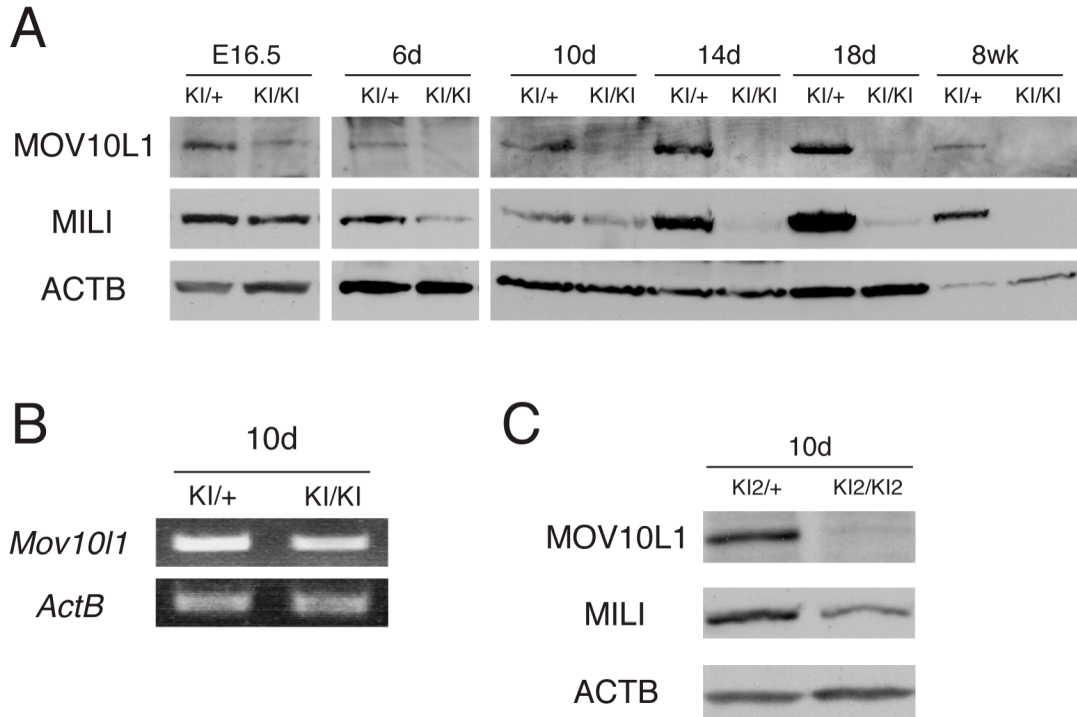
Figure 4.5: MOV10L1 is not expressed in post-natal *Mov10l1*^{KI/KI} and *Mov10l1*^{KI2/KI2} testes. A) Immunoblot analysis of MOV10L1 and MILI in testes from E16.5, 6d (post-natal day 6), 10d, 14d, 18d, and 8 week-old *Mov10l1*^{KI2/+} and *Mov10l1*^{KI2/KI2} mice. ACTB (B-actin) serves as a loading control. **B**) Semi-quantitative RT-PCR analysis of *Mov10l1* transcript abundance in testes from 10d *Mov10l1*^{KI2/+} and *Mov10l1*^{KI2/KI2} mice. *Actb* serves as a loading control. Total RNAs were pre-treated with DNase I. RT-PCR produced no products in controls without reverse transcriptase (data not shown). **C)** Immunoblot analysis of MOV10L1 and MILI in testes from 10d *Mov10l1*^{KI/+} and *Mov10l1*^{KI/KI} mice. ACTB serves as a loading control.
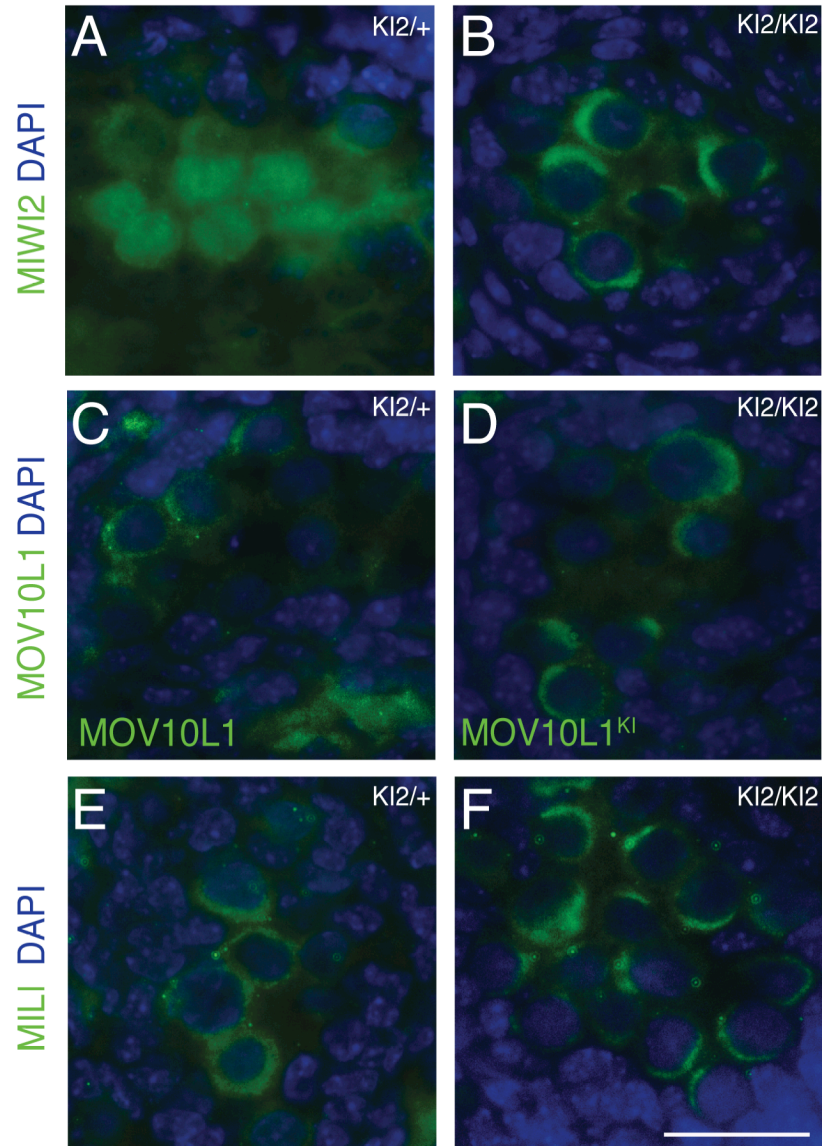
Figure 4.6: Polar conglomeration of piRNA pathway proteins in embryonic
Mov10l1^KI2/KI2 **gonocytes.** Sections of testes from E16.5 *Mov10l1*^KI2/+ and *Mov10l1*^KI2/KI2
embryos were immunostained with antibodies against MIWI2 **(A and B),** MOV10L1 **(C
and D),** and MILI **(E and F)**. DNA was stained with DAPI. Bar, 50 μm.
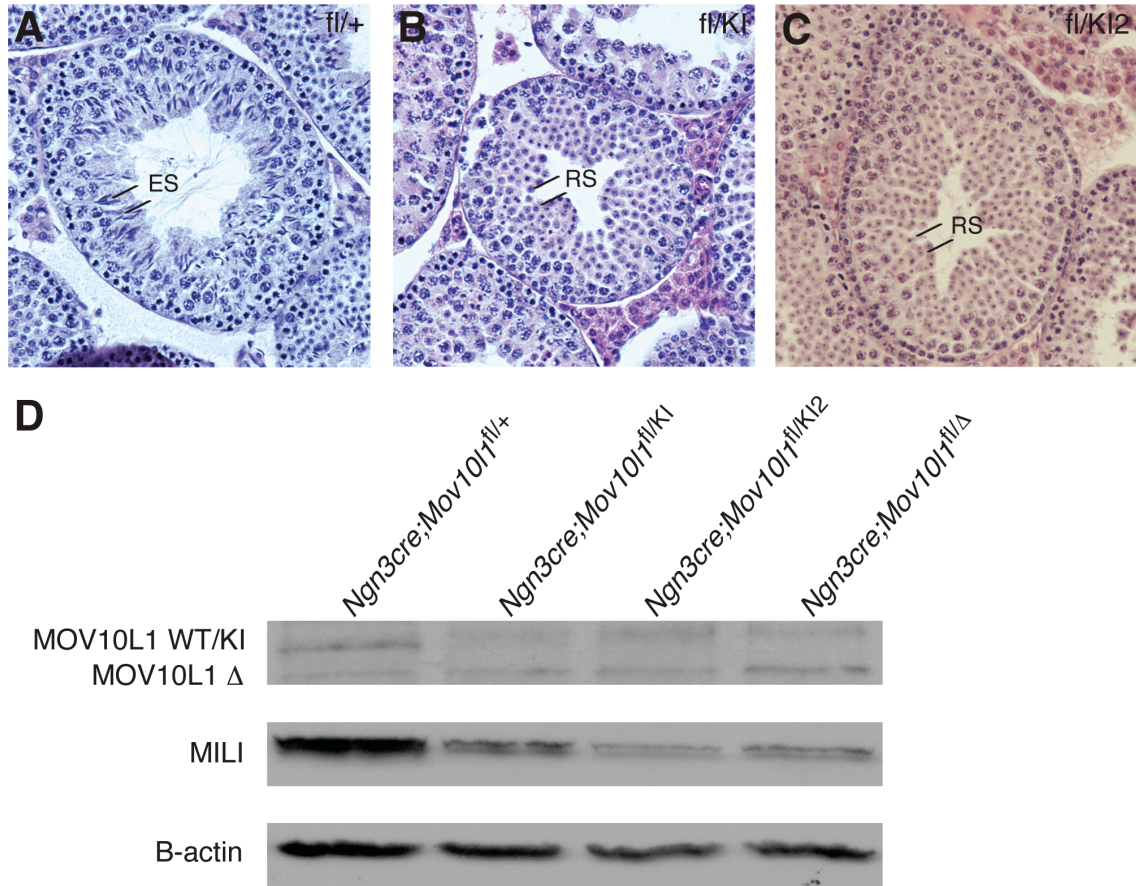
Figure 4.7: Characterizing the requirement for MOV10L1 RNA helicase activity in pachytene piRNA biogenesis. Histology of testes from 8-week-old *Ngn3cre;Mov10l1*^{fl/+} (A), *Ngn3cre;Mov10l1*[KI/fl] (B), and *Ngn3cre;Mov10l1*[KI2/fl] (C) mice. RS, round spermatids; ES, elongating spermatids. **D)** MOV10L1 and MILI expression in testes from 20-day old *Ngn3cre;Mov10l1*^{fl/+}, *Ngn3cre;Mov10l1*[KI/fl], and *Ngn3cre;Mov10l1*[KI2/fl], *Ngn3cre;Mov10l1*[fl/Δ] mice. B-actin serves as a loading control.

CHAPTER 5: CONCLUSIONS AND FUTURE DIRECTIONS

MAJOR CONCLUSIONS

MOV10L1 is a master regulator of piRNA biogenesis and is required for the processing of piRNA precursors, but the exact function of MOV10L1 in piRNA biogenesis remained unclear. The objective of this study was to examine the requirement for MOV10L1 RNA helicase activity in piRNA biogenesis. We determined the requirement for MOV10L1 RNA helicase activity in piRNA biogenesis *in vivo* by characterizing the phenotypes of two knockin mutants containing mutations in residues of the *Mov10l1* ATP binding and ATP hydrolysis motifs that are required for its RNA helicase activity. Pre-pachytene piRNA biogenesis was impaired due to the loss of MOV10L1 ATP binding or MOV10L1 ATP hydrolysis activity. This is supported by the depletion of MILI- and MIWI2-bound pre-pachytene piRNAs, de-repression of TEs, meiotic arrest, and male sterility in both knockin mutants. We also show MOV10L1 ATP binding activity is required for the processing of piRNA precursors. This is supported by the increased expression of pre-pachytene piRNA precursors in the *Mov10l1* ATP binding mutant. This study defines a requirement for MOV10L1 RNA helicase activity in piRNA biogenesis and the processing of piRNA precursors. Combined with previous studies, we envision consecutive rounds of ATP binding and ATP hydrolysis provide the energy for MOV10L1 to translocate along and resolve secondary structures within piRNA precursors. Overall, this study elucidates a novel mechanism required for piRNA biogenesis, spermatogenesis, and male fertility.

62

FUTURE DIRECTIONS: Development of an *in vitro* system for studying mammalian piRNA biogenesis

There are still many unanswered questions in the field of mammalian piRNA biogenesis such as how piRNA precursors are identified by the piRNA processing machinery and how secondary piRNAs are processed. Furthermore, there are many proteins required for mammalian piRNA biogenesis whose functions remain unknown. The development of an *in vitro* system would help to uncover the mechanisms and functions of proteins involved in piRNA biogenesis. An *in vitro* system that is capable of recapitulating piRNA biogenesis has been established in silkworm. Synthetic RNAs are incubated with lysate from BmN4 cells, a silkworm ovarian cell line containing all the components of the piRNA pathway, and a reaction mixture that provides the energy necessary for piRNA processing. Synthetic piRNA intermediates incubated with lysate from BmN4 cells were trimmed into mature piRNAs, and knockdown of Papi and Trimmer inhibited the trimming of synthetic piRNA intermediates (Izumi et al., 2016; Kawaoka et al., 2011). The *in vitro* system in silkworm could be used as a model to develop an *in vitro* system that recapitulates mammalian piRNA biogenesis. While there are no mammalian cell lines that contain all the components of the piRNA pathway, primary tissue such as mouse testes can be used as the source of lysate for the *in vitro* system.

Using the same method as described in Kawaoka et al. 2011, synthetic RNAs whose sequences correspond to piR1 (30nt), a known pachytene piRNA, and a piR1 intermediate (piR1 + 20nt at the 3' end) associated with MILI when incubated in testicular lysate from wildtype mice (Figure 5.1). Furthermore, the piR1 intermediate was processed into an RNA of the same length as piR1 (Figure 5.1). These results show an *in vitro* system using mouse testicular lysate is capable of recapitulating certain aspects

63

of mammalian piRNA biogenesis including the incorporation and trimming of piRNAs and piRNA intermediates. The ability of this system to recapitulate other aspects of mammalian piRNA biogenesis such as the processing of piRNA precursors, preferential incorporation of piRNAs with a 5' uridine residue, and 2'-O-methylation of the 3' ends of piRNAs should be assessed. Finally, piR1 and the piR1 intermediate were still incorporated into MILI and trimmed when incubated in testicular lysate from $Mov10l1^{\Delta/\Delta}$ mice, suggesting that MOV10L1 is not required for the processing of piRNA intermediates or loading of piRNAs onto MILI (Figure 5.1). By incubating different types of synthetic RNAs with testicular lysates from various piRNA pathway mutants, this *in vitro* system can be used to determine the mechanisms and functions of proteins involved in mammalian piRNA biogenesis.

FUTURE DIRECTIONS: Determine the requirement for G-quadruplexes in the processing of piRNA precursors

Additional studies are also required to precisely define how piRNA precursors are processed. Analysis of piRNA precursors in mice revealed an increased potential for secondary structures known as G-quadruplexes to form within regions on piRNA precursors where MOV10L1 binds (Vourekas et al., 2015). This result suggests that G-quadruplexes play a significant role in the processing of piRNA precursors. Furthermore, G-quadruplexes were enriched directly downstream of the 5' ends of piRNAs in multiple mammalian species, suggesting their role in the processing of piRNAs is conserved (Vourekas et al., 2015). G-quadruplexes consist of stacked quartets of guanine residues that are present in DNA and RNA. They form within telomeres in numerous organisms and the promoter regions of many genes including *c-Myc* and chicken *b-globin*, where

64

these structures play roles in DNA transcription, recombination, and replication (Howell et al., 1996; Paeschke et al., 2005; Siddiqui-Jain et al., 2002). G-quadruplexes that form in RNAs have been implicated in translational regulation and alternative splicing (Millevoi et al., 2012).

The requirement for G-quadruplexes in the processing of piRNA precursors can be determined *in vitro* by incubating synthetic piRNA precursors that are enriched for or devoid of G-quadruplexes with lysate from BmN4 cells as described in Kawaoka et al. 2011. However, it should first be confirmed that the enrichment of G-quadruplexes within piRNA precursors is conserved in non-mammalian species. Synthetic piRNA precursors can be designed according to sequence algorithms used to predict for G-quadruplex formation. For example, the sequence algorithm $G_{3+}N_{1-7}G_{3+}N_{1-7}G_{3+}N_{1-7}G_{3+}$, where G corresponded to guanine and N corresponded to any other nucleotide, was used to predict the potential for DNA sequences to form G-quadruplexes in the human genome (Ryvkin et al., 2010). The BG4 antibody, which specifically recognized DNA and RNA G-quadruplexes in human cells, can be used to assess the ability for the synthetic piRNA precursors to form G-quadruplexes *in vitro* (Biffi et al., 2013; Biffi et al., 2014). The requirement for G-quadruplexes in the processing of piRNA precursors can also be determined *in vivo* by generating mice in which the guanine residues directly downstream of the 5' end of piR1 are mutated. If G-quadruplexes are essential for the processing of piRNA precursors, piR1 should be depleted and the piR1 precursor should accumulate in the mutant mice. piR1 can be detected using Northern blot analysis, and piR1 precursor expression can be measured using qRT-PCR. This study could elucidate a conserved mechanism underlying the processing of piRNA precursors.

FUTURE DIRECTIONS: MOV10L1 as a target for potential male contraceptives

The percentage of unplanned pregnancies worldwide in 2012 was staggering according to the study performed in Sedgh et al. 2014. While there are many effective birth control options for females, there is currently a lack of male contraceptive options, resulting in a higher rate of unplanned pregnancies. The most accessible male contraceptive options are vasectomy and condoms; however, both vasectomy and condoms have their limitations. Condoms have a relatively high failure rate, and vasectomies can cause unwanted immunological consequences and become less reversible with time (Nieschlag et al., 2011; Schwingl and Guess, 2000). There are also several testosterone-based therapies in clinical trials. However, the effects of hormonal therapies vary based on the individual with up to one-third of individuals requiring an additional agent (Nieschlag et al., 2011). Hormonal therapies can also affect other physiological functions and cause unwanted side effects with prolonged use (Mathew and Bantwal, 2012). Another potential male contraceptive option is a small molecule inhibitor that can target proteins essential for spermatogenesis and male fertility. JQ1, a BRDT inhibitor, occupies an acetyl-lysine pocket on the testis-specific protein BRDT (Matzuk et al., 2012). JQ1 crossed the blood:testis barrier, inhibited sperm generation and motility, did not cause any changes in hormone levels, and its effects were completely reversible (Matzuk et al., 2012). However, JQ1 is not being used in human clinical trials because of its short half-life (Zuber et al., 2011).

As a testis-specific protein that is required for spermatogenesis and male sterility, MOV10L1 is a promising target for male contraceptives. In this study, we show MOV10L1 RNA helicase activity is required for spermatogenesis and male fertility. The feasibility of targeting residues essential for RNA helicase activity has been shown by the development of small molecule inhibitors such as RK-33 that targets the ATP-binding

66

cleft of DDX3 and ML216 that targets the DNA-binding cleft of BLM (Bol et al., 2015; Nguyen et al., 2013). Therefore, small molecule inhibitors that target residues required for MOV10L1 RNA helicase activity have the potential to be effective male contraceptives. Additional sites for targeting include residues of MOV10L1 that are required for its interaction with other components of the piRNA pathway. The development of an effective male contraceptive would undoubtedly lower the rate of unplanned pregnancies and improve global health.

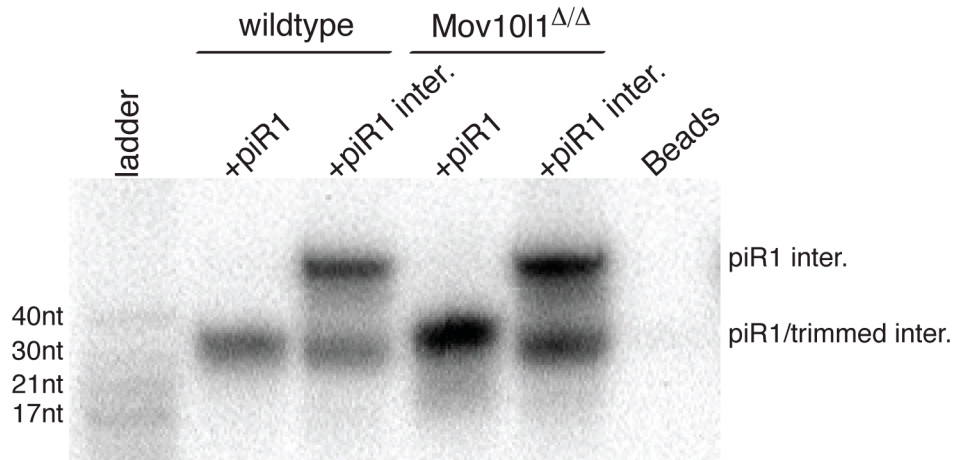**FIGURES**

Figure 5.1: Trimming and incorporation of synthetic RNAs into MILI *in vitro.*
Synthetic RNAs were radiolabeled and incubated with testicular lysate from wildtype or
Mov10l1^{Δ/Δ} mice and a reaction mixture. The MILI complex was immunoprecipitated from
the lysate. RNAs were extracted from the MILI complex and visualized using UREA-
PAGE followed by autoradiography.

68

REFERENCES

Aravin, A., Gaidatzis, D., Pfeffer, S., Lagos-Quintana, M., Landgraf, P., Iovino, N., Morris, P., Brownstein, M.J., Kuramochi-Miyagawa, S., Nakano, T., *et al.* (2006). A novel class of small RNAs bind to MILI protein in mouse testes. Nature *442,* 203-207.

Aravin, A.A., Sachidanandam, R., Bourc'his, D., Schaefer, C., Pezic, D., Toth, K.F., Bestor, T., and Hannon, G.J. (2008). A piRNA pathway primed by individual transposons is linked to de novo DNA methylation in mice. Mol. Cell *31,* 785-799.

Aravin, A.A., Sachidanandam, R., Girard, A., Fejes-Toth, K., and Hannon, G.J. (2007). Developmentally regulated piRNA clusters implicate MILI in transposon control. Science *316,* 744-747.

Aravin, A.A., van der Heijden, G.W., Castaneda, J., Vagin, V.V., Hannon, G.J., and Bortvin, A. (2009). Cytoplasmic compartmentalization of the fetal piRNA pathway in mice. PLoS Genet. *5,* e1000764.

Baker, J.A., Buck, G.M., Vena, J.E., and Moysich, K.B. (2005). Fertility patterns prior to testicular cancer diagnosis. Cancer Causes Control *16,* 295-299.

Belancio, V.P., Hedges, D.J., and Deininger, P. (2008). Mammalian non-LTR retrotransposons: for better or worse, in sickness and in health. Genome Res. *18,* 343-358.

Biffi, G., Di Antonio, M., Tannahill, D., and Balasubramanian, S. (2014). Visualization and selective chemical targeting of RNA G-quadruplex structures in the cytoplasm of human cells. Nat. Chem. *6,* 75-80.

Biffi, G., Tannahill, D., McCafferty, J., and Balasubramanian, S. (2013). Quantitative visualization of DNA G-quadruplex structures in human cells. Nat. Chem. *5,* 182-186.

Bol, G.M., Vesuna, F., Xie, M., Zeng, J., Aziz, K., Gandhi, N., Levine, A., Irving, A., Korz, D., Tantravedi, S., *et al.* (2015). Targeting DDX3 with a small molecule inhibitor for lung cancer therapy. EMBO Mol. Med. *7,* 648-669.

Brennecke, J., Aravin, A.A., Stark, A., Dus, M., Kellis, M., Sachidanandam, R., and Hannon, G.J. (2007). Discrete small RNA-generating loci as master regulators of transposon activity in Drosophila. Cell *128,* 1089-1103.

Carmell, M.A., Girard, A., van de Kant, H.J., Bourc'his, D., Bestor, T.H., de Rooij, D.G., and Hannon, G.J. (2007). MIWI2 is essential for spermatogenesis and repression of transposons in the mouse male germline. Dev. Cell. *12,* 503-514.

Castaneda, J., Genzor, P., van der Heijden, G.W., Sarkeshik, A., Yates, J.R.,3rd, Ingolia, N.T., and Bortvin, A. (2014). Reduced pachytene piRNAs and translation underlie spermiogenic arrest in Maelstrom mutant mice. Embo j. *33,* 1999-2019.

69

Chandra, A., Copen, C.E., and Stephen, E.H. (2013). Infertility and impaired fecundity in the United States, 1982-2010: data from the National Survey of Family Growth. Natl. Health. Stat. Report *(67),* 1-18, 1 p following 19.

Chuma, S., Hosokawa, M., Kitamura, K., Kasai, S., Fujioka, M., Hiyoshi, M., Takamune, K., Noce, T., and Nakatsuji, N. (2006). Tdrd1/Mtr-1, a tudor-related gene, is essential for male germ-cell differentiation and nuage/germinal granule formation in mice. Proc. Natl. Acad. Sci. U. S. A. *103,* 15894-15899.

Clermont, Y. (1972). Kinetics of spermatogenesis in mammals: seminiferous epithelium cycle and spermatogonial renewal. Physiol. Rev. *52,* 198-236.

Culty, M. (2013). Gonocytes, from the fifties to the present: is there a reason to change the name? Biol. Reprod. *89,* 46.

De Fazio, S., Bartonicek, N., Di Giacomo, M., Abreu-Goodger, C., Sankar, A., Funaya, C., Antony, C., Moreira, P.N., Enright, A.J., and O'Carroll, D. (2011). The endonuclease activity of Mili fuels piRNA amplification that silences LINE1 elements. Nature *480,* 259-263.

de Kretser, D.M., Loveland, K.L., Meinhardt, A., Simorangkir, D., and Wreford, N. (1998). Spermatogenesis. Hum. Reprod. *13 Suppl 1,* 1-8.

Deng, W., and Lin, H. (2002). Miwi, a Murine Homolog of Piwi, Encodes a Cytoplasmic Protein Essential for Spermatogenesis. Dev. Cell. *2,* 819-830.

Di Giacomo, M., Comazzetto, S., Saini, H., De Fazio, S., Carrieri, C., Morgan, M., Vasiliauskaite, L., Benes, V., Enright, A.J., and O'Carroll, D. (2013). Multiple epigenetic mechanisms and the piRNA pathway enforce LINE1 silencing during adult spermatogenesis. Mol. Cell *50,* 601-608.

Fairman-Williams, M.E., Guenther, U.P., and Jankowsky, E. (2010). SF1 and SF2 helicases: family matters. Curr. Opin. Struct. Biol. *20,* 313-324.

Frost, R.J., Hamra, F.K., Richardson, J.A., Qi, X., Bassel-Duby, R., and Olson, E.N. (2010). MOV10L1 is necessary for protection of spermatocytes against retrotransposons by Piwi-interacting RNAs. Proc. Natl. Acad. Sci. U. S. A. *107,* 11847-11852.

Fu, Q., and Wang, P.J. (2014). Mammalian piRNAs: Biogenesis, function, and mysteries. Spermatogenesis *4,* e27889.

Ginsburg, M., Snow, M.H., and McLaren, A. (1990). Primordial germ cells in the mouse embryo during gastrulation. Development *110,* 521-528.

Girard, A., Sachidanandam, R., Hannon, G.J., and Carmell, M.A. (2006). A germline-specific class of small RNAs binds mammalian Piwi proteins. Nature *442,* 199-202.

Goh, W.S., Falciatori, I., Tam, O.H., Burgess, R., Meikar, O., Kotaja, N., Hammell, M., and Hannon, G.J. (2015). piRNA-directed cleavage of meiotic transcripts regulates spermatogenesis. Genes Dev. *29,* 1032-1044.

Goodier, J.L., and Kazazian, H.H.,Jr. (2008). Retrotransposons revisited: the restraint and rehabilitation of parasites. Cell *135,* 23-35.

Gou, L.T., Dai, P., Yang, J.H., Xue, Y., Hu, Y.P., Zhou, Y., Kang, J.Y., Wang, X., Li, H., Hua, M.M.*, et al.* (2014). Pachytene piRNAs instruct massive mRNA elimination during late spermiogenesis. Cell Res. *24,* 680-700.

Grivna, S.T., Beyret, E., Wang, Z., and Lin, H. (2006). A novel class of small RNAs in mouse spermatogenic cells. Genes Dev. *20,* 1709-1714.

Gunawardane, L.S., Saito, K., Nishida, K.M., Miyoshi, K., Kawamura, Y., Nagami, T., Siomi, H., and Siomi, M.C. (2007). A slicer-mediated mechanism for repeat-associated siRNA 5' end formation in Drosophila. Science *315,* 1587-1590.

Hajkova, P., Erhardt, S., Lane, N., Haaf, T., El-Maarri, O., Reik, W., Walter, J., and Surani, M.A. (2002). Epigenetic reprogramming in mouse primordial germ cells. Mech. Dev. *117,* 15-23.

Han, B.W., Wang, W., Li, C., Weng, Z., and Zamore, P.D. (2015). Noncoding RNA. piRNA-guided transposon cleavage initiates Zucchini-dependent, phased piRNA production. Science *348,* 817-821.

Hock, J., and Meister, G. (2008). The Argonaute protein family. Genome Biol. *9,* 210-2008-9-2-210. Epub 2008 Feb 26.

Houwing, S., Kamminga, L.M., Berezikov, E., Cronembold, D., Girard, A., van den Elst, H., Filippov, D.V., Blaser, H., Raz, E., Moens, C.B.*, et al.* (2007). A role for Piwi and piRNAs in germ cell maintenance and transposon silencing in Zebrafish. Cell *129,* 69-82.

Howell, R.M., Woodford, K.J., Weitzmann, M.N., and Usdin, K. (1996). The chicken beta-globin gene promoter forms a novel "cinched" tetrahelical structure. J. Biol. Chem. *271,* 5208-5214.

Ipsaro, J.J., Haase, A.D., Knott, S.R., Joshua-Tor, L., and Hannon, G.J. (2012). The structural biochemistry of Zucchini implicates it as a nuclease in piRNA biogenesis. Nature *491,* 279-283.

Izumi, N., Shoji, K., Sakaguchi, Y., Honda, S., Kirino, Y., Suzuki, T., Katsuma, S., and Tomari, Y. (2016). Identification and Functional Analysis of the Pre-piRNA 3' Trimmer in Silkworms. Cell *164,* 962-973.

Jankowsky, E. (2011). RNA helicases at work: binding and rearranging. Trends Biochem. Sci. *36,* 19-29.

Jensen, T.K., Jacobsen, R., Christensen, K., Nielsen, N.C., and Bostofte, E. (2009). Good semen quality and life expectancy: a cohort study of 43,277 men. Am. J. Epidemiol. *170,* 559-565.

Jorgensen, N., Vierula, M., Jacobsen, R., Pukkala, E., Perheentupa, A., Virtanen, H.E., Skakkebaek, N.E., and Toppari, J. (2011). Recent adverse trends in semen quality and testis cancer incidence among Finnish men. Int. J. Androl. *34,* e37-48.

Kawaoka, S., Izumi, N., Katsuma, S., and Tomari, Y. (2011). 3' end formation of PIWI-interacting RNAs in vitro. Mol. Cell *43,* 1015-1022.

Khurana, J.S., and Theurkauf, W.E. (2008). piRNA function in germline development. In StemBook, (Cambridge (MA): Jaspreet S. Khurana and William E. Theurkauf)

Kocer, A., Reichmann, J., Best, D., and Adams, I.R. (2009). Germ cell sex determination in mammals. Mol. Hum. Reprod. *15,* 205-213.

Kuramochi-Miyagawa, S., Kimura, T., Ijiri, T.W., Isobe, T., Asada, N., Fujita, Y., Ikawa, M., Iwai, N., Okabe, M., Deng, W.*, et al.* (2004). Mili, a mammalian member of piwi family gene, is essential for spermatogenesis. Development *131,* 839-849.

Kuramochi-Miyagawa, S., Watanabe, T., Gotoh, K., Takamatsu, K., Chuma, S., Kojima-Kita, K., Shiromoto, Y., Asada, N., Toyoda, A., Fujiyama, A.*, et al.* (2010). MVH in piRNA processing and gene silencing of retrotransposons. Genes Dev. *24,* 887-892.

Kuramochi-Miyagawa, S., Watanabe, T., Gotoh, K., Totoki, Y., Toyoda, A., Ikawa, M., Asada, N., Kojima, K., Yamaguchi, Y., Ijiri, T.W.*, et al.* (2008). DNA methylation of retrotransposon genes is regulated by Piwi family members MILI and MIWI2 in murine fetal testes. Genes Dev. *22,* 908-917.

Lander, E.S., Linton, L.M., Birren, B., Nusbaum, C., Zody, M.C., Baldwin, J., Devon, K., Dewar, K., Doyle, M., FitzHugh, W.*, et al.* (2001). Initial sequencing and analysis of the human genome. Nature *409,* 860-921.

Li, X.Z., Roy, C.K., Dong, X., Bolcun-Filas, E., Wang, J., Han, B.W., Xu, J., Moore, M.J., Schimenti, J.C., Weng, Z., and Zamore, P.D. (2013). An ancient transcription factor initiates the burst of piRNA production during early meiosis in mouse testes. Mol. Cell *50,* 67-81.

Lim, A.K., Lorthongpanich, C., Chew, T.G., Tan, C.W., Shue, Y.T., Balu, S., Gounko, N., Kuramochi-Miyagawa, S., Matzuk, M.M., Chuma, S.*, et al.* (2013). The nuage mediates retrotransposon silencing in mouse primordial ovarian follicles. Development *140,* 3819-3825.

Lim, S.L., Qu, Z.P., Kortschak, R.D., Lawrence, D.M., Geoghegan, J., Hempfling, A.L., Bergmann, M., Goodnow, C.C., Ormandy, C.J., Wong, L.*, et al.* (2015). HENMT1 and piRNA Stability Are Required for Adult Male Germ Cell Transposon Repression and to Define the Spermatogenic Program in the Mouse. PLoS Genet. *11,* e1005620.

Manakov, S.A., Pezic, D., Marinov, G.K., Pastor, W.A., Sachidanandam, R., and Aravin, A.A. (2015). MIWI2 and MILI Have Differential Effects on piRNA Biogenesis and DNA Methylation. Cell. Rep. *12,* 1234-1243.

Martin, S.L., and Branciforte, D. (1993). Synchronous expression of LINE-1 RNA and protein in mouse embryonal carcinoma cells. Mol. Cell. Biol. *13,* 5383-5392.

Martinez, J., and Tuschl, T. (2004). RISC is a 5' phosphomonoester-producing RNA endonuclease. Genes Dev. *18,* 975-980.

Mascarenhas, M.N., Flaxman, S.R., Boerma, T., Vanderpoel, S., and Stevens, G.A. (2012). National, regional, and global trends in infertility prevalence since 1990: a systematic analysis of 277 health surveys. PLoS Med. *9,* e1001356.

Mathew, V., and Bantwal, G. (2012). Male contraception. Indian. J. Endocrinol. Metab. *16,* 910-917.

Matzuk, M.M., McKeown, M.R., Filippakopoulos, P., Li, Q., Ma, L., Agno, J.E., Lemieux, M.E., Picaud, S., Yu, R.N., Qi, J., Knapp, S., and Bradner, J.E. (2012). Small-molecule inhibition of BRDT for male contraception. Cell *150,* 673-684.

Meikar, O., Da Ros, M., Korhonen, H., and Kotaja, N. (2011). Chromatoid body and small RNAs in male germ cells. Reproduction *142,* 195-209.

Millevoi, S., Moine, H., and Vagner, S. (2012). G-quadruplexes in RNA biology. Wiley Interdiscip. Rev. RNA *3,* 495-507.

Mohn, F., Handler, D., and Brennecke, J. (2015). Noncoding RNA. piRNA-guided slicing specifies transcripts for Zucchini-dependent, phased piRNA biogenesis. Science *348,* 812-817.

Molyneaux, K.A., Stallock, J., Schaible, K., and Wylie, C. (2001). Time-lapse analysis of living mouse germ cell migration. Dev. Biol. *240,* 488-498.

Mouse Genome Sequencing Consortium, Waterston, R.H., Lindblad-Toh, K., Birney, E., Rogers, J., Abril, J.F., Agarwal, P., Agarwala, R., Ainscough, R., Alexandersson, M.*, et al.* (2002). Initial sequencing and comparative analysis of the mouse genome. Nature *420,* 520-562.

Moyes, D., Griffiths, D.J., and Venables, P.J. (2007). Insertional polymorphisms: a new lease of life for endogenous retroviruses in human disease. Trends Genet. *23,* 326-333.

Nguyen, G.H., Dexheimer, T.S., Rosenthal, A.S., Chu, W.K., Singh, D.K., Mosedale, G., Bachrati, C.Z., Schultz, L., Sakurai, M., Savitsky, P.*, et al.* (2013). A small molecule inhibitor of the BLM helicase modulates chromosome stability in human cells. Chem. Biol. *20,* 55-62.

Nieschlag, E., Vorona, E., Wenk, M., Hemker, A.K., Kamischke, A., and Zitzmann, M. (2011). Hormonal male contraception in men with normal and subnormal semen parameters. Int. J. Androl. *34,* 556-567.

Nishimasu, H., Ishizu, H., Saito, K., Fukuhara, S., Kamatani, M.K., Bonnefond, L., Matsumoto, N., Nishizawa, T., Nakanaga, K., Aoki, J*., et al.* (2012). Structure and function of Zucchini endoribonuclease in piRNA biogenesis. Nature *491,* 284-287.

Ostertag, E.M., and Kazazian, H.H.,Jr. (2001). Biology of mammalian L1 retrotransposons. Annu. Rev. Genet. *35,* 501-538.

Paeschke, K., Simonsson, T., Postberg, J., Rhodes, D., and Lipps, H.J. (2005). Telomere end-binding proteins control the formation of G-quadruplex DNA structures in vivo. Nat. Struct. Mol. Biol. *12,* 847-854.

Rashid, U.J., Paterok, D., Koglin, A., Gohlke, H., Piehler, J., and Chen, J.C. (2007). Structure of Aquifex aeolicus argonaute highlights conformational flexibility of the PAZ domain as a potential regulator of RNA-induced silencing complex function. J. Biol. Chem. *282,* 13824-13832.

Reuter, M., Berninger, P., Chuma, S., Shah, H., Hosokawa, M., Funaya, C., Antony, C., Sachidanandam, R., and Pillai, R.S. (2011). Miwi catalysis is required for piRNA amplification-independent LINE1 transposon silencing. Nature *480,* 264-267.

Rivas, F.V., Tolia, N.H., Song, J.J., Aragon, J.P., Liu, J., Hannon, G.J., and Joshua-Tor, L. (2005). Purified Argonaute2 and an siRNA form recombinant human RISC. Nat. Struct. Mol. Biol. *12,* 340-349.

Rives, N., Perdrix, A., Hennebicq, S., Saias-Magnan, J., Melin, M.C., Berthaut, I., Barthelemy, C., Daudin, M., Szerman, E., Bresson, J.L., Brugnon, F., and Bujan, L. (2012). The semen quality of 1158 men with testicular cancer at the time of cryopreservation: results of the French National CECOS Network. J. Androl. *33,* 1394-1401.

Roeder, G.S., and Bailis, J.M. (2000). The pachytene checkpoint. Trends Genet. *16,* 395-403.

Ryvkin, P., Hershman, S.G., Wang, L.S., and Johnson, F.B. (2010). Computational approaches to the detection and analysis of sequences with intramolecular G-quadruplex forming potential. Methods Mol. Biol. *608,* 39-50.

Saito, K., Ishizu, H., Komai, M., Kotani, H., Kawamura, Y., Nishida, K.M., Siomi, H., and Siomi, M.C. (2010). Roles for the Yb body components Armitage and Yb in primary piRNA biogenesis in Drosophila. Genes Dev. *24,* 2493-2498.

Sasaki, H., and Matsui, Y. (2008). Epigenetic events in mammalian germ-cell development: reprogramming and beyond. Nat. Rev. Genet. *9,* 129-140.

Saxe, J.P., Chen, M., Zhao, H., and Lin, H. (2013). Tdrkh is essential for spermatogenesis and participates in primary piRNA biogenesis in the germline. Embo j. *32,* 1869-1885.

Schwingl, P.J., and Guess, H.A. (2000). Safety and effectiveness of vasectomy. Fertil. Steril. *73,* 923-936.

Sedgh, G., Singh, S., and Hussain, R. (2014). Intended and unintended pregnancies worldwide in 2012 and recent trends. Stud. Fam. Plann. *45,* 301-314.

Siddiqui-Jain, A., Grand, C.L., Bearss, D.J., and Hurley, L.H. (2002). Direct evidence for a G-quadruplex in a promoter region and its targeting with a small molecule to repress c-MYC transcription. Proc. Natl. Acad. Sci. U. S. A. *99,* 11593-11598.

Smallwood, S.A., and Kelsey, G. (2012). De novo DNA methylation: a germ cell perspective. Trends Genet. *28,* 33-42.

Song, J.J., Smith, S.K., Hannon, G.J., and Joshua-Tor, L. (2004). Crystal structure of Argonaute and its implications for RISC slicer activity. Science *305,* 1434-1437.

Soper, S.F., van der Heijden, G.W., Hardiman, T.C., Goodheart, M., Martin, S.L., de Boer, P., and Bortvin, A. (2008). Mouse maelstrom, a component of nuage, is essential for spermatogenesis and transposon repression in meiosis. Dev. Cell. *15,* 285-297.

Tanner, N.K., and Linder, P. (2001). DExD/H box RNA helicases: from generic motors to specific dissociation functions. Mol. Cell *8,* 251-262.

Theophilus, B.D., Enayat, M.S., Higuchi, M., Kazazian, H.H., Antonarakis, S.E., and Hill, F.G. (1998). Independent occurrence of the novel Arg2163 to His mutation in the factor VIII gene in three unrelated families with haemophila A with different phenotypes. Mutations in brief no. 126. Online. Hum. Mutat. *11,* 334.

Vagin, V.V., Sigova, A., Li, C., Seitz, H., Gvozdev, V., and Zamore, P.D. (2006). A distinct small RNA pathway silences selfish genetic elements in the germline. Science *313,* 320-324.

Vourekas, A., Zheng, K., Fu, Q., Maragkakis, M., Alexiou, P., Ma, J., Pillai, R.S., Mourelatos, Z., and Wang, P.J. (2015). The RNA helicase MOV10L1 binds piRNA precursors to initiate piRNA processing. Genes Dev. *29,* 617-629.

Vourekas, A., Zheng, Q., Alexiou, P., Maragkakis, M., Kirino, Y., Gregory, B.D., and Mourelatos, Z. (2012). Mili and Miwi target RNA repertoire reveals piRNA biogenesis and function of Miwi in spermiogenesis. Nat. Struct. Mol. Biol. *19,* 773-781.

Watanabe, T., Chuma, S., Yamamoto, Y., Kuramochi-Miyagawa, S., Totoki, Y., Toyoda, A., Hoki, Y., Fujiyama, A., Shibata, T., Sado, T.*, et al.* (2011). MITOPLD is a mitochondrial protein essential for nuage formation and piRNA biogenesis in the mouse germline. Dev. Cell. *20,* 364-375.

Weng, Y., Czaplinski, K., and Peltz, S.W. (1998). ATP is a cofactor of the Upf1 protein that modulates its translation termination and RNA binding activities. Rna *4,* 205-214.

Weng, Y., Czaplinski, K., and Peltz, S.W. (1996). Genetic and biochemical characterization of mutations in the ATPase and helicase regions of the Upf1 protein. Mol. Cell. Biol. *16,* 5477-5490.

Yang, F., and Wang, P.J. (2016). Multiple LINEs of retrotransposon silencing mechanisms in the mammalian germline. Semin. Cell Dev. Biol.

Yoshida, S., Sukeno, M., Nakagawa, T., Ohbo, K., Nagamatsu, G., Suda, T., and Nabeshima, Y. (2006). The first round of mouse spermatogenesis is a distinctive program that lacks the self-renewing spermatogonia stage. Development *133,* 1495-1505.

Yuan, Y.R., Pei, Y., Ma, J.B., Kuryavyi, V., Zhadina, M., Meister, G., Chen, H.Y., Dauter, Z., Tuschl, T., and Patel, D.J. (2005). Crystal structure of A. aeolicus argonaute, a site-specific DNA-guided endoribonuclease, provides insights into RISC-mediated mRNA cleavage. Mol. Cell *19,* 405-419.

Zamudio, N., Barau, J., Teissandier, A., Walter, M., Borsos, M., Servant, N., and Bourc'his, D. (2015). DNA methylation restrains transposons from adopting a chromatin signature permissive for meiotic recombination. Genes Dev. *29,* 1256-1270.

Zamudio, N., and Bourc'his, D. (2010). Transposable elements in the mammalian germline: a comfortable niche or a deadly trap? Heredity (Edinb) *105,* 92-104.

Zhang, P., Kang, J.Y., Gou, L.T., Wang, J., Xue, Y., Skogerboe, G., Dai, P., Huang, D.W., Chen, R., Fu, X.D., Liu, M.F., and He, S. (2015). MIWI and piRNA-mediated cleavage of messenger RNAs in mouse testes. Cell Res. *25,* 193-207.

Zhang, Y., Maksakova, I.A., Gagnier, L., van de Lagemaat, L.N., and Mager, D.L. (2008). Genome-wide assessments reveal extremely high levels of polymorphism of two active families of mouse endogenous retroviral elements. PLoS Genet. *4,* e1000007.

Zhao, S., Gou, L.T., Zhang, M., Zu, L.D., Hua, M.M., Hua, Y., Shi, H.J., Li, Y., Li, J., Li, D., Wang, E.D., and Liu, M.F. (2013). piRNA-triggered MIWI ubiquitination and removal by APC/C in late spermatogenesis. Dev. Cell. *24,* 13-25.

Zheng, K., and Wang, P.J. (2012). Blockade of pachytene piRNA biogenesis reveals a novel requirement for maintaining post-meiotic germline genome integrity. PLoS Genet. *8,* e1003038.

Zheng, K., Xiol, J., Reuter, M., Eckardt, S., Leu, N.A., McLaughlin, K.J., Stark, A., Sachidanandam, R., Pillai, R.S., and Wang, P.J. (2010). Mouse MOV10L1 associates with Piwi proteins and is an essential component of the Piwi-interacting RNA (piRNA) pathway. Proc. Natl. Acad. Sci. U. S. A. *107,* 11841-11846.

Zickler, D., and Kleckner, N. (1999). Meiotic chromosomes: integrating structure and function. Annu. Rev. Genet. *33,* 603-754.

Zuber, J., Shi, J., Wang, E., Rappaport, A.R., Herrmann, H., Sison, E.A., Magoon, D., Qi, J., Blatt, K., Wunderlich, M.*, et al.* (2011). RNAi screen identifies Brd4 as a therapeutic target in acute myeloid leukaemia. Nature *478,* 524-528.